Sensitivity of Wind Turbine Airfoil Sections to Geometry Variations Inherent in Modular Blades

Ken Brown, Nick Molinaro, Tim Meyers, Mike Nelson, Aurelien Borgoltz, Nanya Intaratep, William Devenport

Virginia Tech, Blacksburg, VA, U.S.A.

Jonathan Luedke, David Pesetsky

GE Power and Water, Greenville, SC, U.S.A.

June 9, 2015
NAWEA Symposium

The information, data, or work presented herein was funded in part by the Advanced Research Projects Agency-Energy (ARPA-E), U.S. Department of Energy, under Award Number DE-AR0000293.

CREATe
Virginia Tech Center for Renewable Energy and Aerodynamic Testing

Motivation

Wind turbine blades need to grow longer to lower the cost of electricity

CREATe
Virginia Tech Center for Renewable Energy and Aerodynamic Testing

Conventional

Modular

Photo: courtesy of GE Power and Water

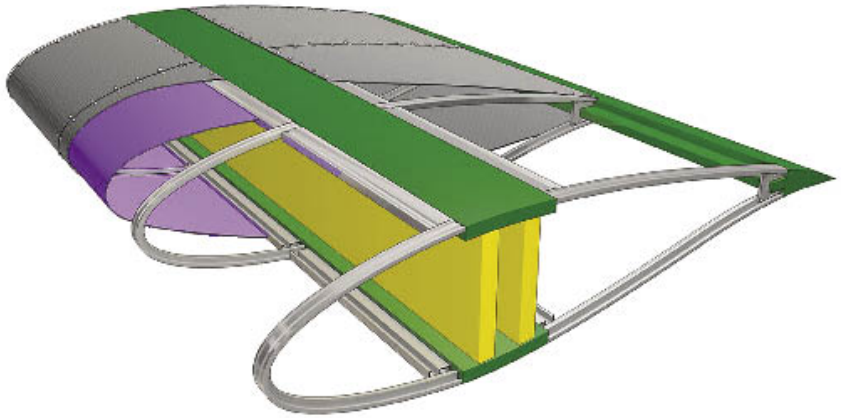

2-piece mold shell manufacturing → **Modular manufacturing**

Transportation difficulties → **Build on-site**

Low stiffness/weight ratio → **Tailor-able stiffness/weight ratio**

Fixed outer mold line → **Misaligned/flexible outer mold line**

Dutton *et al*. (2000), Vionis *et al*. (2006), Saenz *et al*. (2014)

Outline

CREATe
Virginia Tech Center for Renewable Energy and Aerodynamic Testing

Modular wind turbine blades

Misaligned sections

- Literature
- Configuration
- Test setup
- Results

Fabric sections

- Literature
- Configuration
- Test setup
- Results

Summary

Misaligned sections: literature

Transition behavior

2D disturbances thought to contribute to Tollmein-Schlichting type transition (Braslow, 1960)

Roughness Reynolds number: $Re_k = \mu_k k u_k / \nu_k$

- u_k - flow velocity at top of roughness in undisturbed ca
- k - roughness height
- ν_k - kinematic viscosity at roughness location

Study	Geometry	$Re_{k,critical}$
Fage (1943)	Flat/arched ridge	204-240
Smith and Clutter (1959)	Spanwise wires	40-260
Drake *et al.* (2010)	Forward-facing step	150-2,100
Drake *et al.* (2010)	Backward-facing step	75-800
Current study	Backward- and forward-facing ramp	?

$Re_{k,critical}$ may be influenced by length of preceding laminar boundary layer, width of geometric feature, type of the geometric feature, and pressure gradient in boundary layer

Misaligned sections: configuration

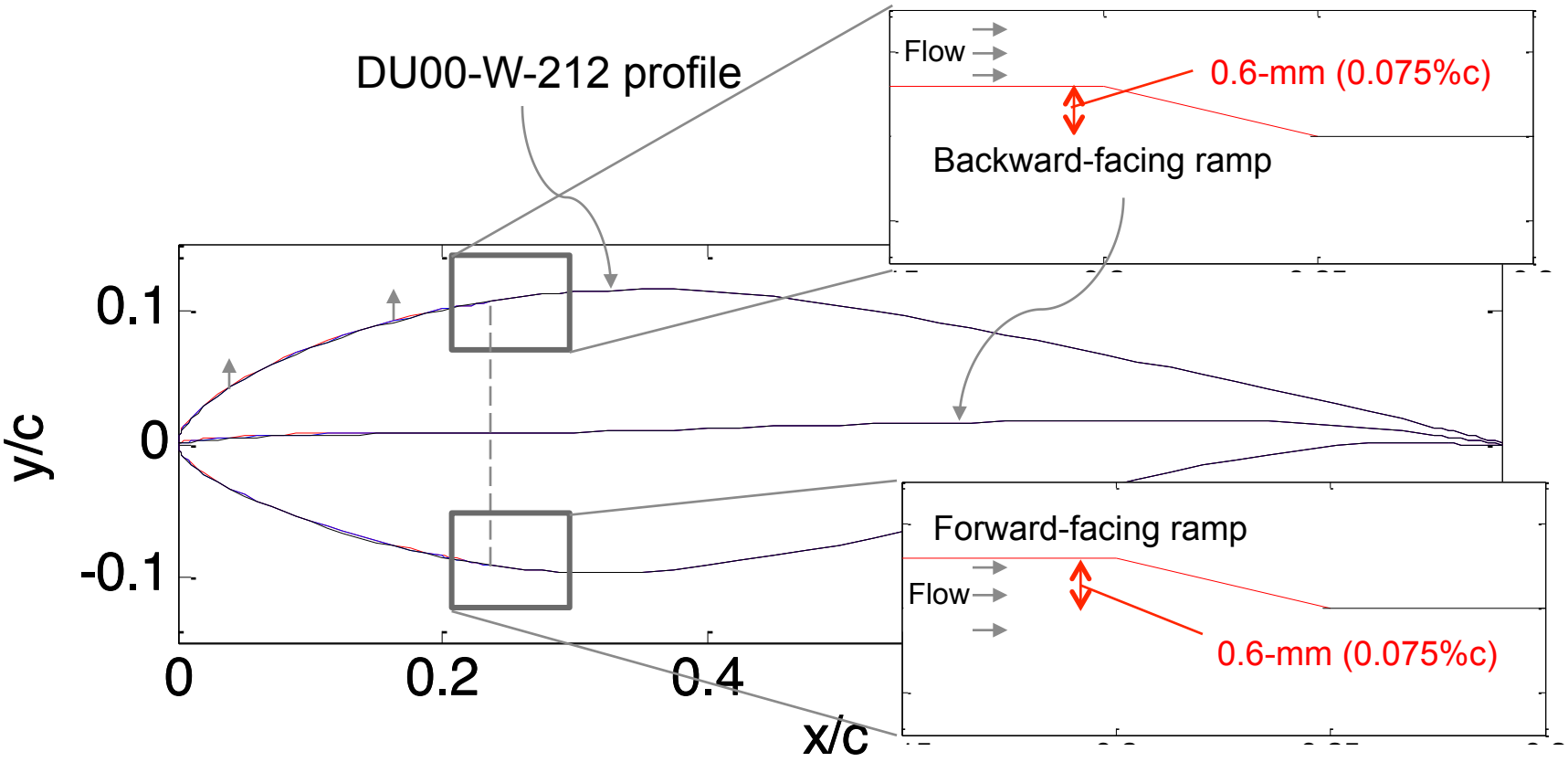

Offset results in an effective increase in camber
and, more importantly, produce discontinuities in the profile

Misaligned sections: test setup

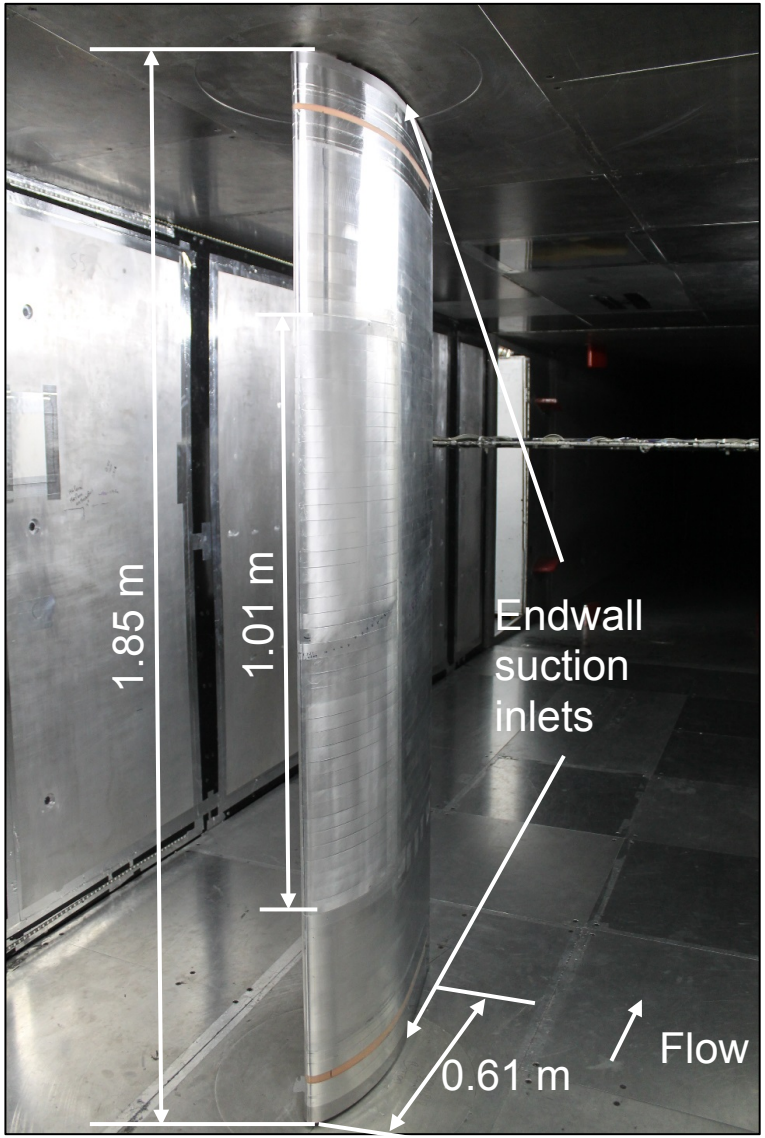

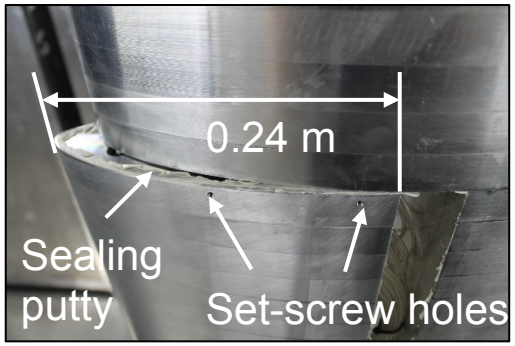

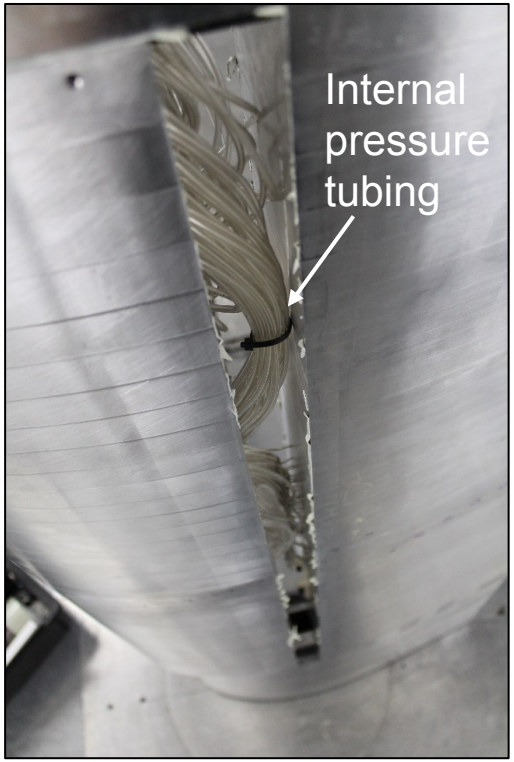

Model:

- DU00-W-212
- 0.6-m chord
- 64 aluminum laminates
- 73 pressure taps
- 3 nose modules: baseline, 0.3-, and 0.6-mm offsets
- Endwall suction on

Measurements:

- Mean surface pressure
- Wake profiles

Test Conditions:

- $Re = 2.5 \times 10^6$
- $Ma = 0.21$

Misaligned sections: results

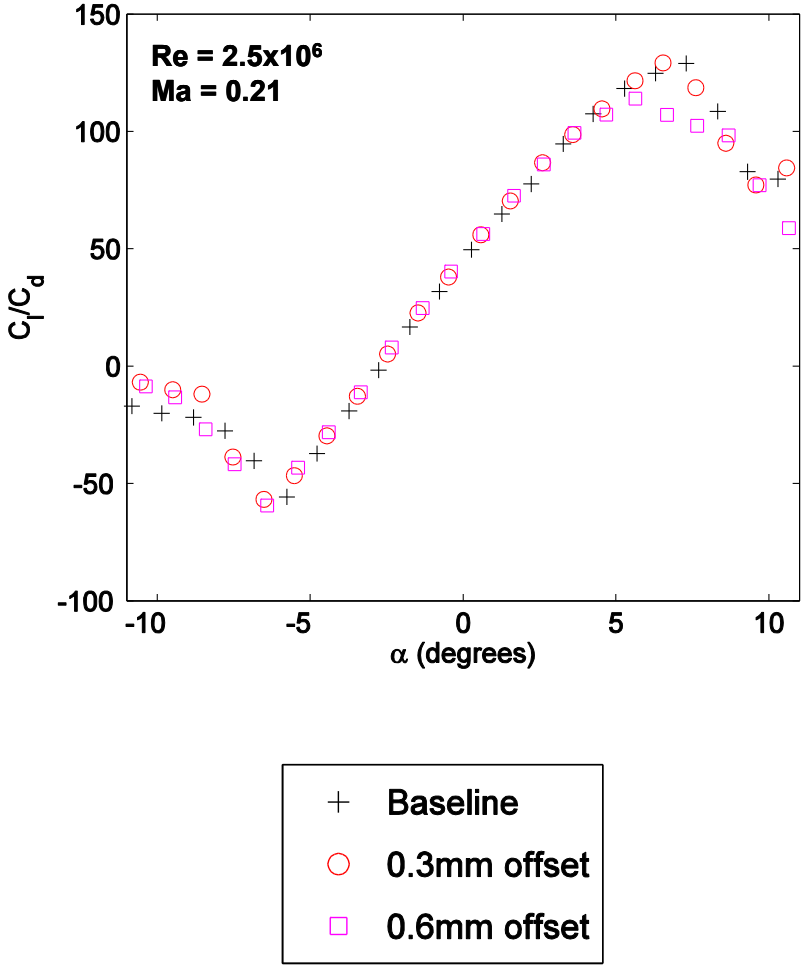

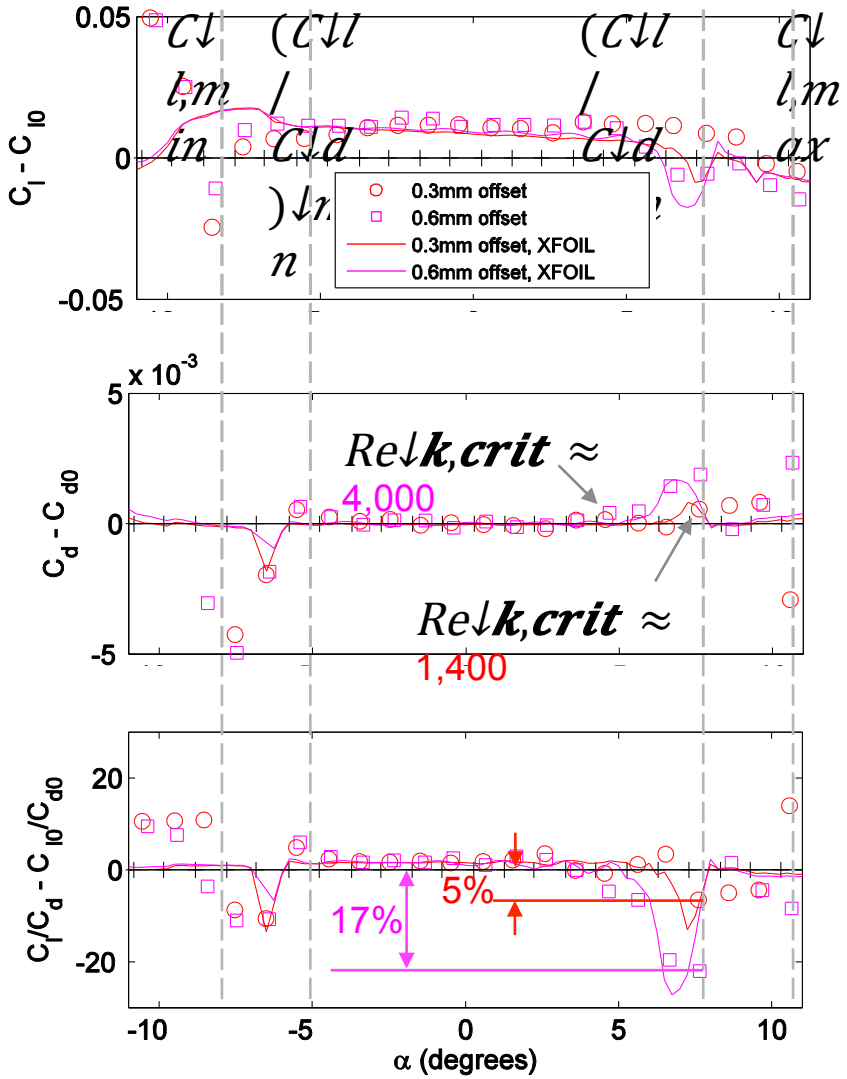

Misaligned sections: results

XFOIL transition prediction

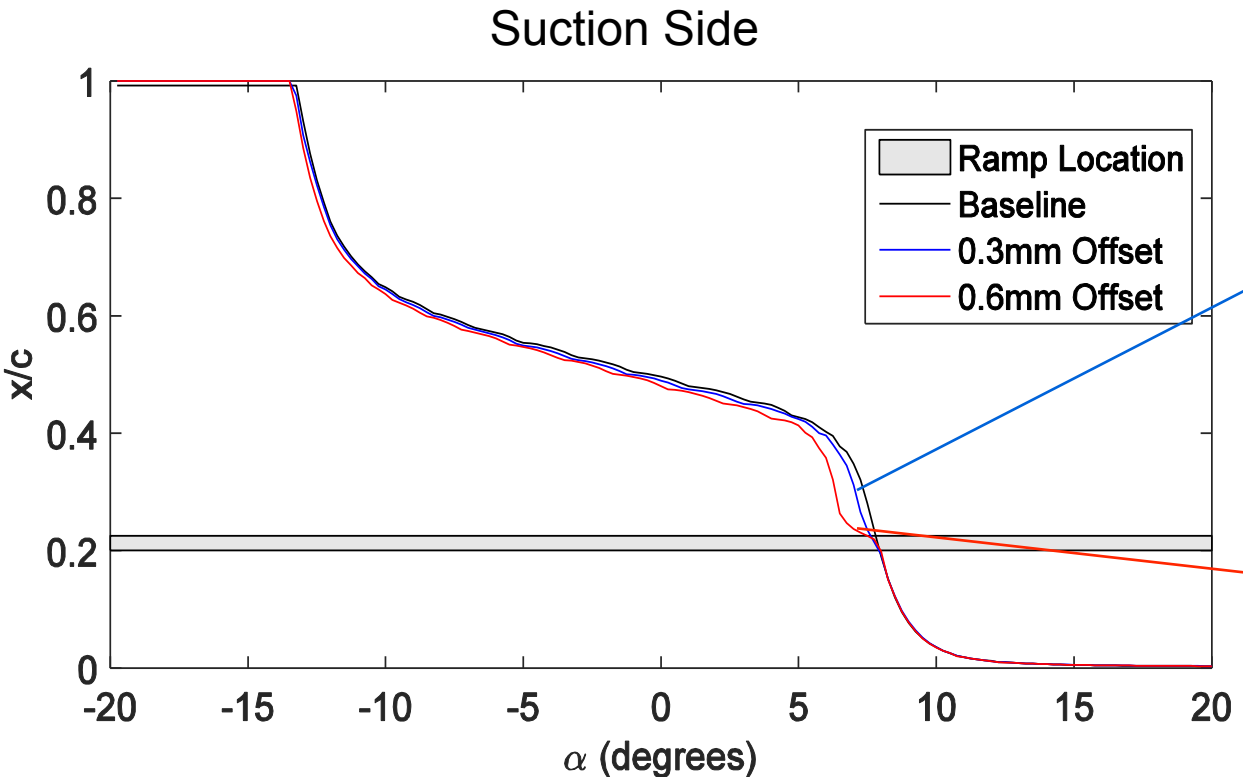

0.3-mm offset:
5.5% jump in transition location at design angle

0.6-mm offset:
12.1% jump in transition location at design angle

Boundary layer predictions from XFOIL support premature transition hypothesis

Fabric sections: literature

Micro-aerial vehicle wings:

Low-aspect ratio, low Reynolds number, single-membrane wings

Increased camber increases C_l and C_d; overall effect of these changes producing a C_l/C_d comparable to similar rigid wings

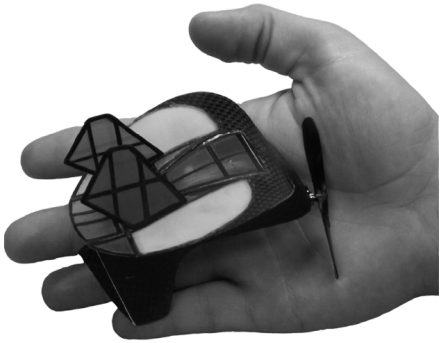

Stanford *et al.* (2007)

Princeton sailwing:

Higher aspect ratio, high Reynolds number, double-membrane wings

Lift curve nonlinear due to the changes in induced tension in the membrane with angle of attack

Predicted C_l/C_d ratio for flexible wing similar to that of rigid wing and even exceeding in certain cases

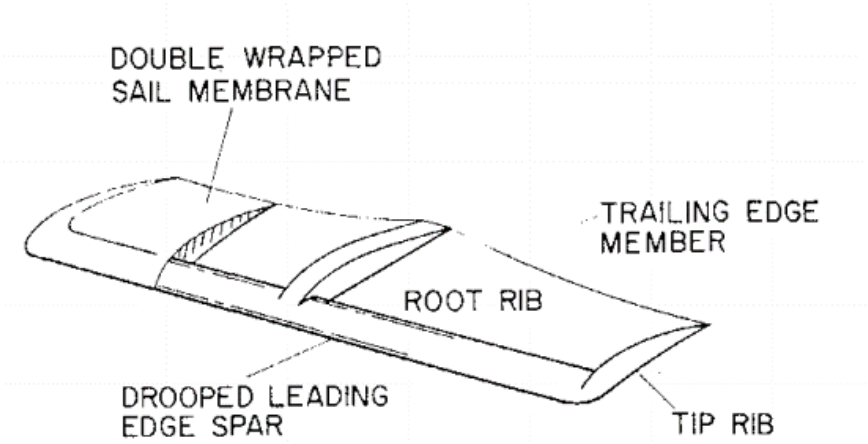

Ormiston (1971)

Fabric section: configuration

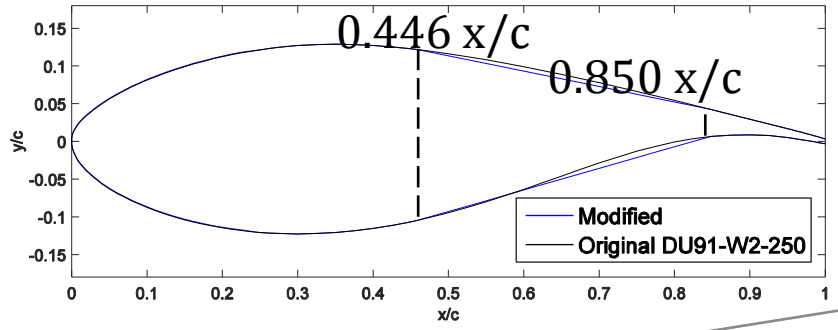

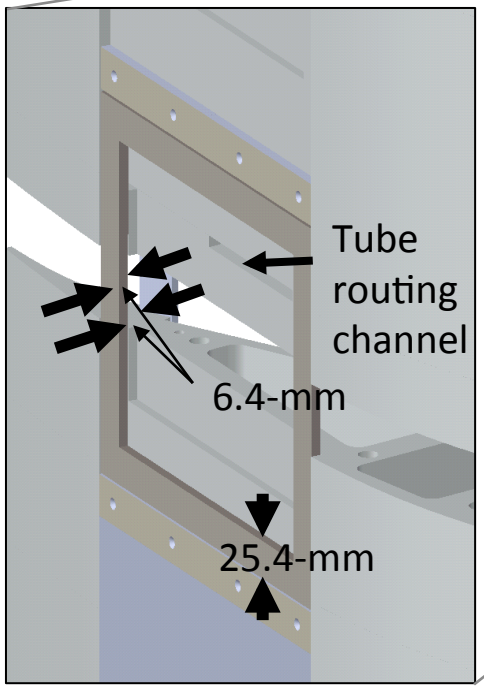

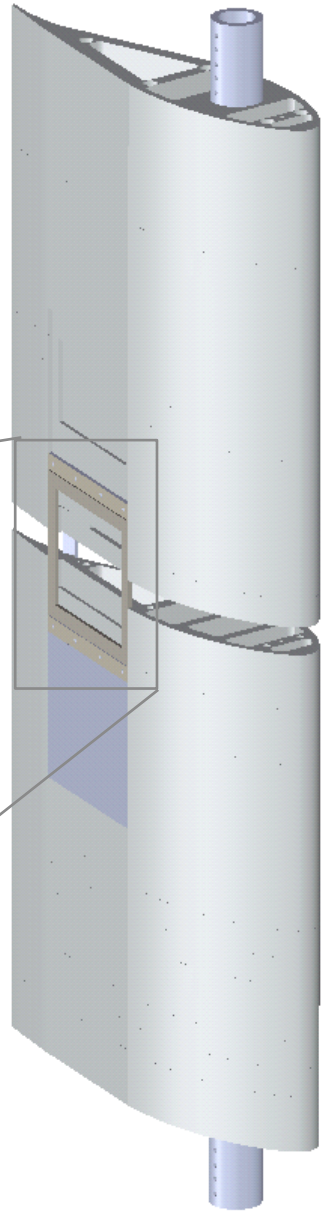

Fabric section: test setup

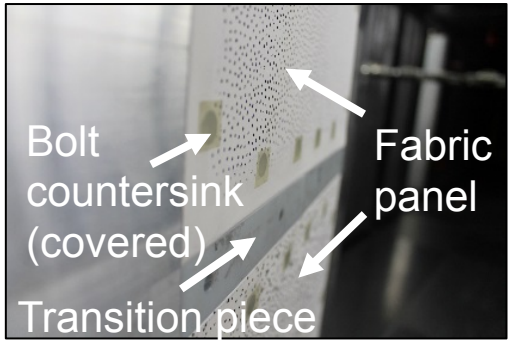

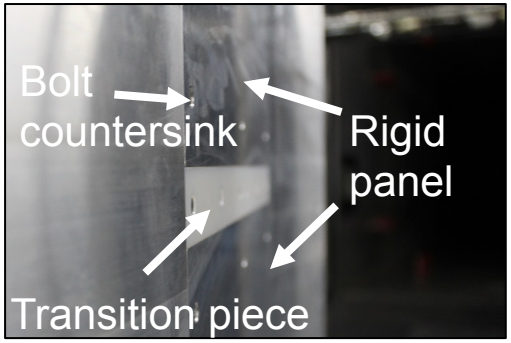

Model:

- Modified DU91-W2-250
- 0.8-m chord
- 34 aluminum laminates
- 64 pressure taps
- 6 removable panels (3 suction side, 3 pressure side)
- No endwall suction

Measurements:

- Mean surface pressure
- Wake profiles
- Fabric deflection (DIC)

Test Conditions:

- Re = 2.5 - 3.0x10^6
- Ma = 0.15 - 0.19

Fabric sections: results

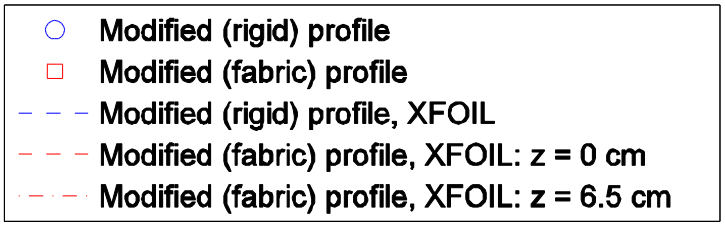

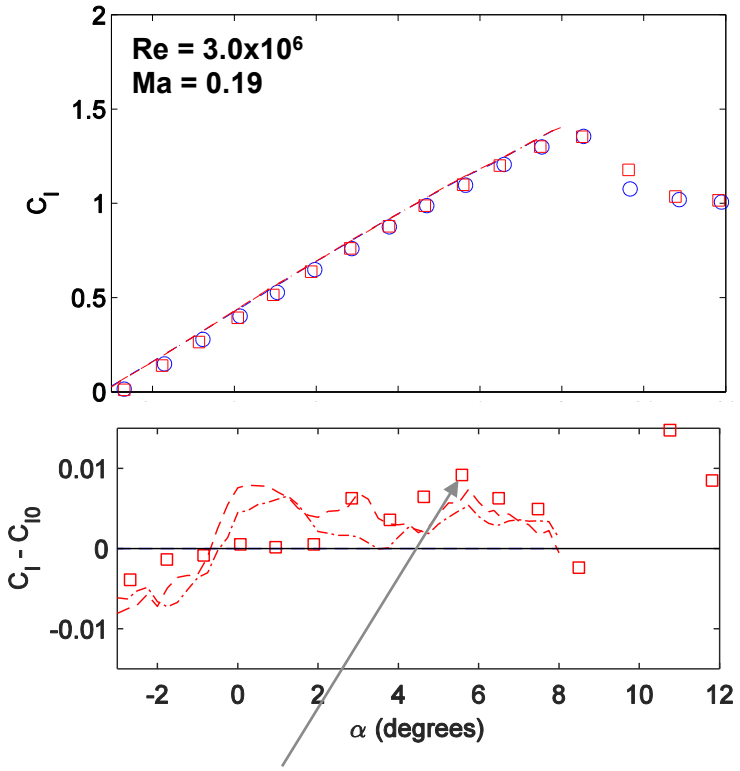

0.8% higher C_l at design angle of attack

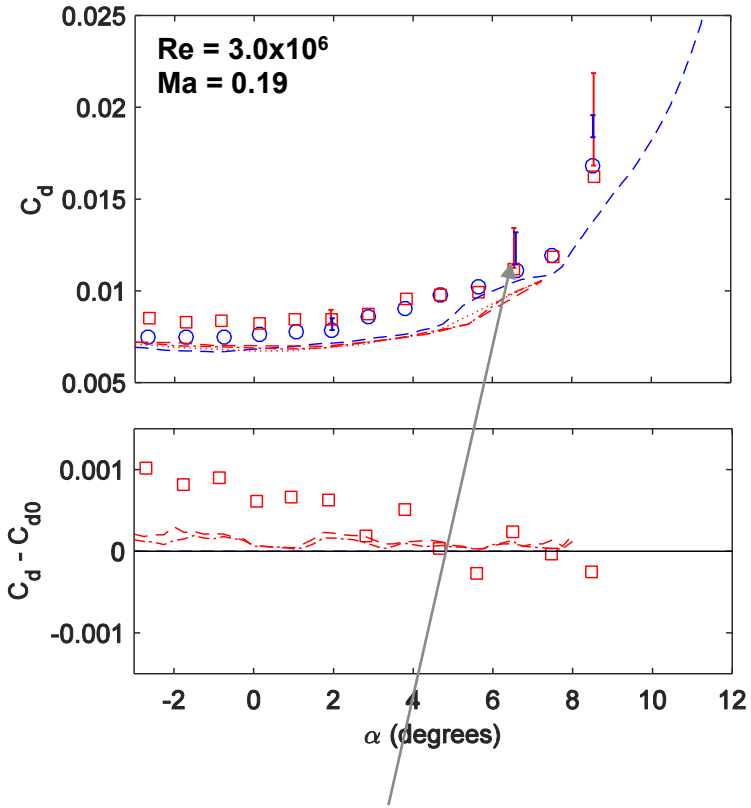

19% variation in spanwise drag

Fabric sections: results

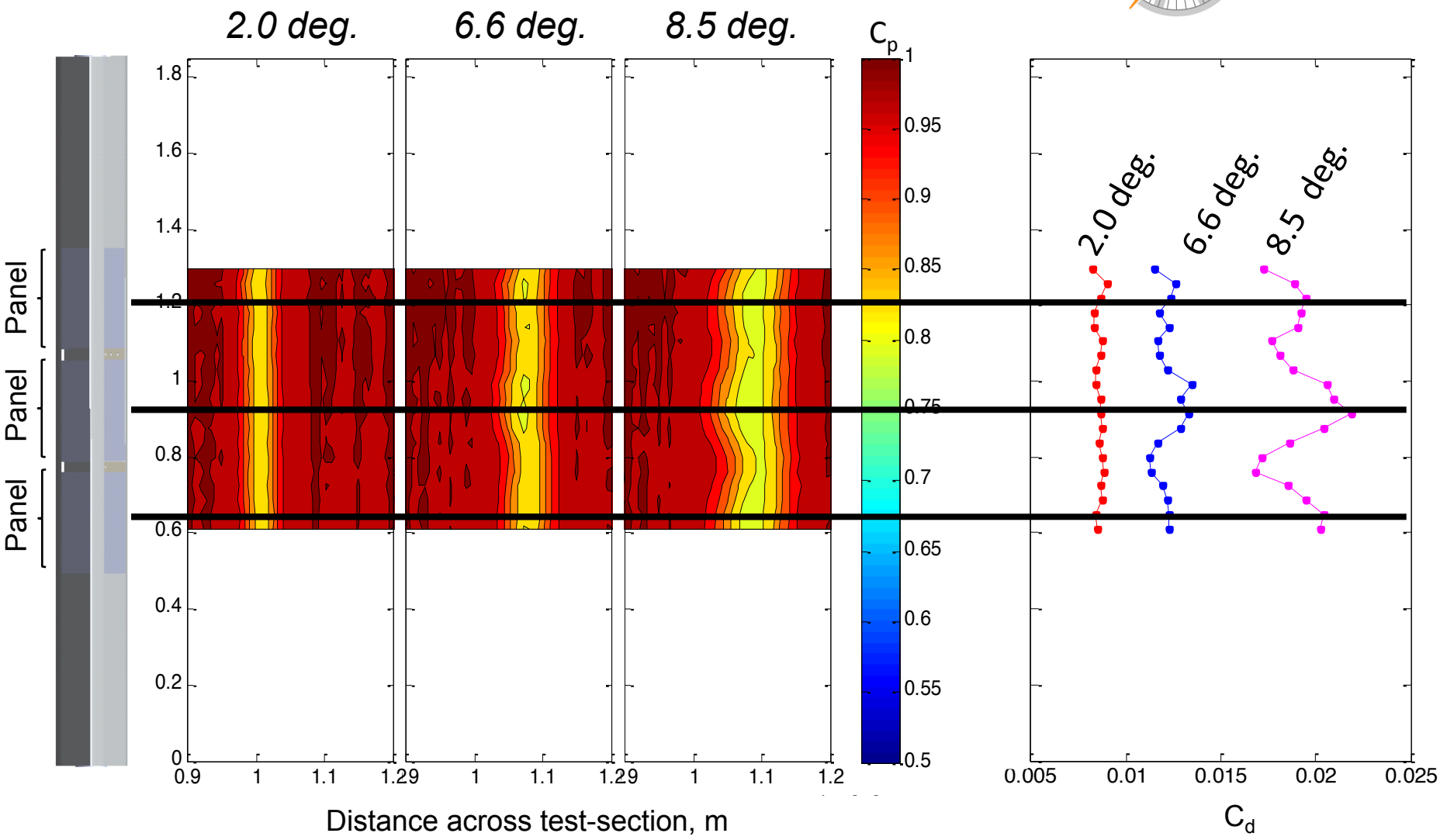

Fabric flexibility produces spanwise drag variation

Fabric sections: results

Suction side deflection

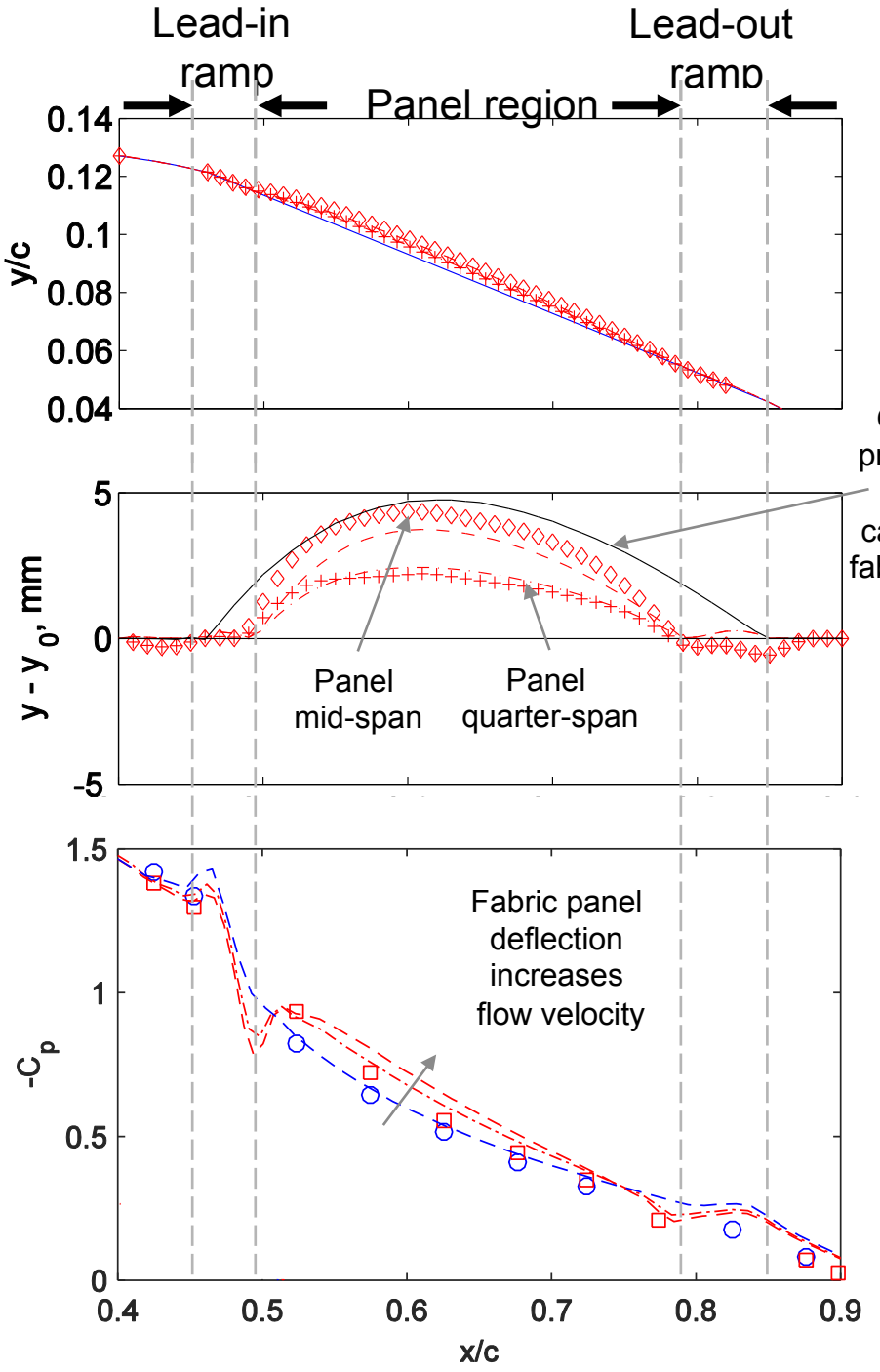

Original profile has similar camber to fabric profile

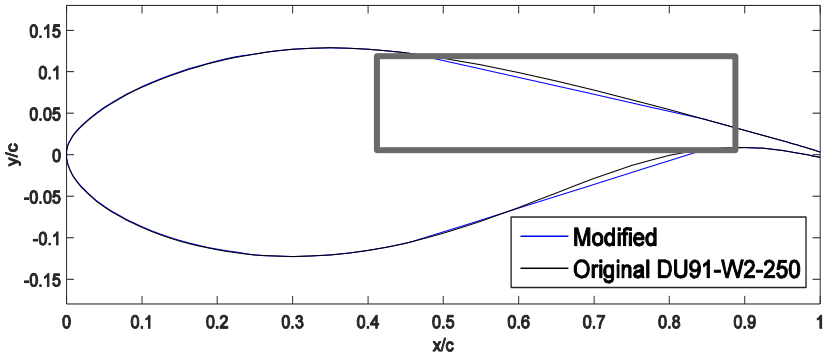

- Modified (rigid) panels
- Modified (fabric) panels: z = 0 cm
- Modified (fabric) panels: z = 6.5 cm
- Modified (fabric) panels, XFOIL: z = 0 cm
- Modified (fabric) panels, XFOIL: z = 6.5 cm

- Modified (rigid) profile, α=6.59°
- Modified (fabric) profile, α=6.59°
- Modified (rigid) profile, XFOIL, α=6.38°
- Modified (fabric) profile, XFOIL: z = 0 cm, α=6.38°
- Modified (fabric) profile, XFOIL: z = 6.5 cm, α=6.38°

Summary/Conclusions

CREATe
Virginia Tech Center for Renewable Energy and Aerodynamic Testing

Misaligned model:

- Small variation (<1%) in linear region lift due to effective camber increase
- Premature transition responsible for increased drag and $(C\downarrow l/C\downarrow d)\downarrow max$ decrease of ~5% for a typical misalignment and ~17% for severe misalignment

Fabric model:

- 0.8% increase in $C\downarrow l$ for fabric versus baseline model at $(C\downarrow l/C\downarrow d)\downarrow max$ and above due to camber increase
- Large spanwise variation in drag due to fabric deflection requires detailed spanwise measurement
- Deflected fabric shape is not far from baseline shape, at least on suction side
- Fabric models afford opportunity for tuning performance with fabric properties

Thank you!

References

[1]Dutton, A., Kildegaard, C., Dobbe, T., Bensoussan, R., Kensche, C., Hahn, F., van Delft, D., and de Winkel, G., "Design, structural design, structural testing, and cost effectiveness of sectional wind turbine blades. (Publishable Final Report)," Tech. rep., The European Commission, 2000.

[2]Vionis, P., Lekou, D., Gonzalez, F., Mieres, J., Kossivas, T., Soria, E., Gutierrez, E., Galiotis, C., Philippidis, T., Voutsinas, S., and Hofmann, D., "Development of a MW scale wind turbine for high wind complex terrain sites; the MEGAWIND project." Tech. rep., 2006 European Wind Energy Conference, 2006.

[3]Saenz, E., Nuin, I., Montejo, R., and Sanz, J., "Development and validation of a new joint system for sectional blades," *Wind Energy*, Vol. 18, No. 3, 2014, pp. 419428.

[6]Braslow, A. L., "Review of the effect of distributed surface roughness on boundary-layer transition," Tech. rep., DTIC Document, 1960.

[7]Fage, A., "The smallest size of a spanwise surface corrugation which affects boundary-layer transition on an aerofoil," *HM Stationery Office*, 1943.

[8]Smith, A., "The smallest height of roughness capable of affecting boundary-layer transition," *Journal of the Aerospace Sciences*, Vol. 26, No. 4, 1959, pp. 229–245.

[10]Drake, A., Bender, A. M., Korntheuer, A., Westphal, R. V., McKeon, B. J., Gerashchenko, S., Rohe, W., and Dale, G., "Step Excrescence Effects for Manufacturing Tolerances on Laminar Flow Wings," *AIAA Paper*, Vol. 375, 2010.

[18]Stanford, B., Sytsma, M., Albertani, R., Viieru, D., Shyy, W., and Ifju, P., "Static aeroelastic model validation of membrane micro air vehicle wings," *AIAA journal*, Vol. 45, No. 12, 2007, pp. 2828–2837.

[19]Ormiston, R. A., "Theoretical and experimental aerodynamics of the sailwing," *Journal of Aircraft*, Vol. 8, No. 2, 1971, pp. 77–84.


CREATe
Virginia Tech Center for Renewable
Energy and Aerodynamic Testing

DU00

Misaligned sections: literature

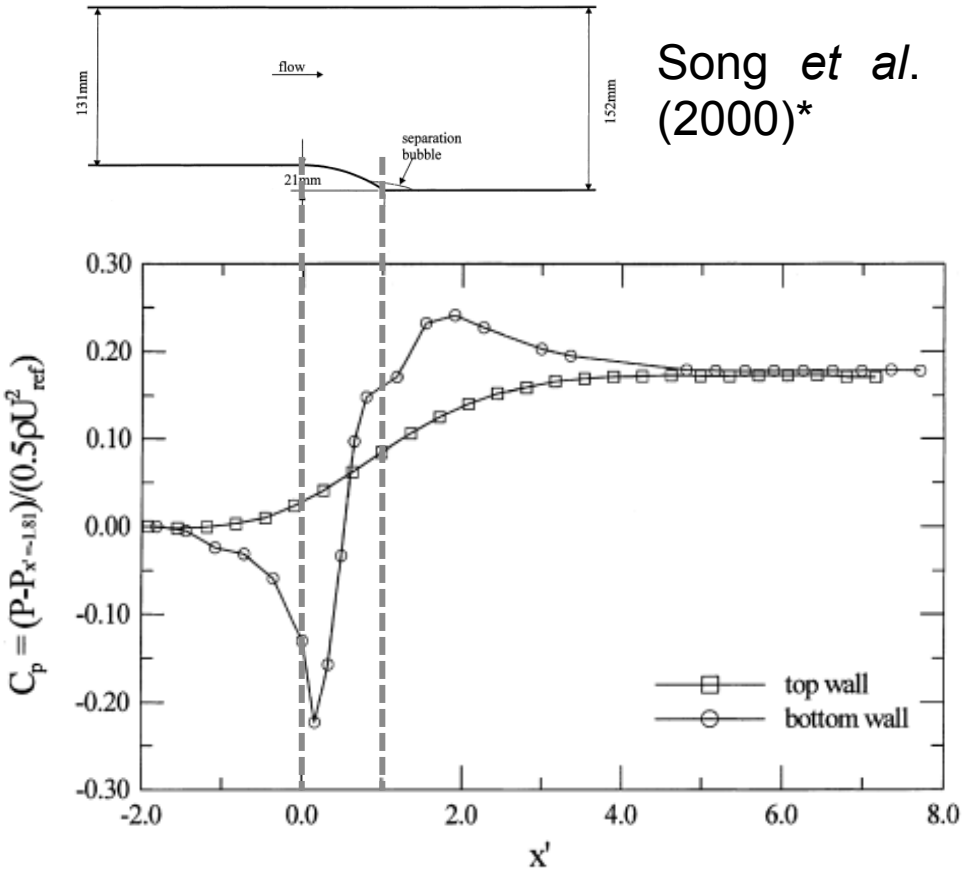

Song *et al.* (2000)*

*Song *et al.* (2000) - Experimental study of a separating, reattaching, and redeveloping flow over a smoothly contoured ramp

Misaligned sections: setup

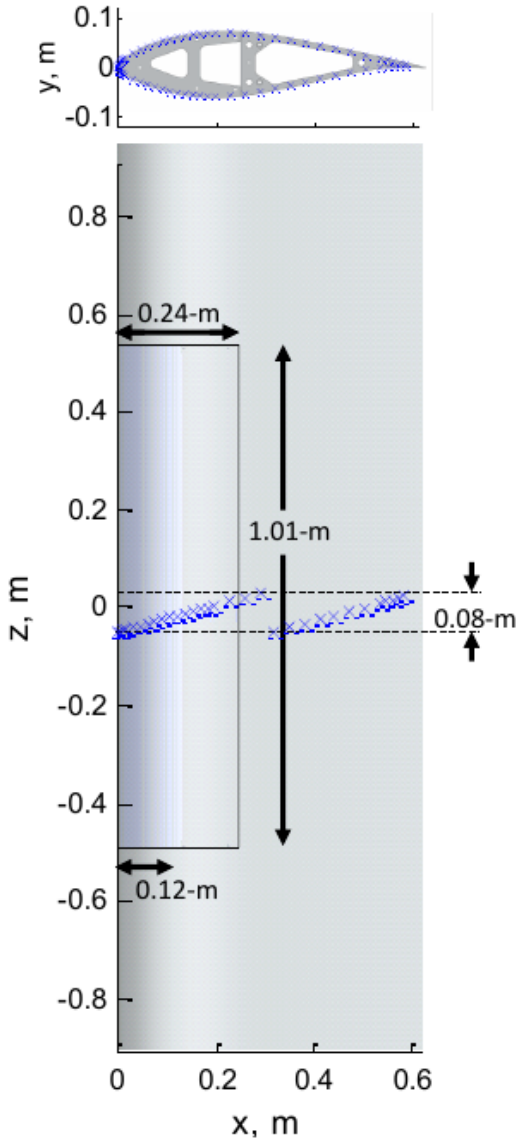

Effective Angle of Attack Increase

Offset profile looks as if at higher angle of attack

Lowering the angle of attack by 0.06 deg. makes differences minimal

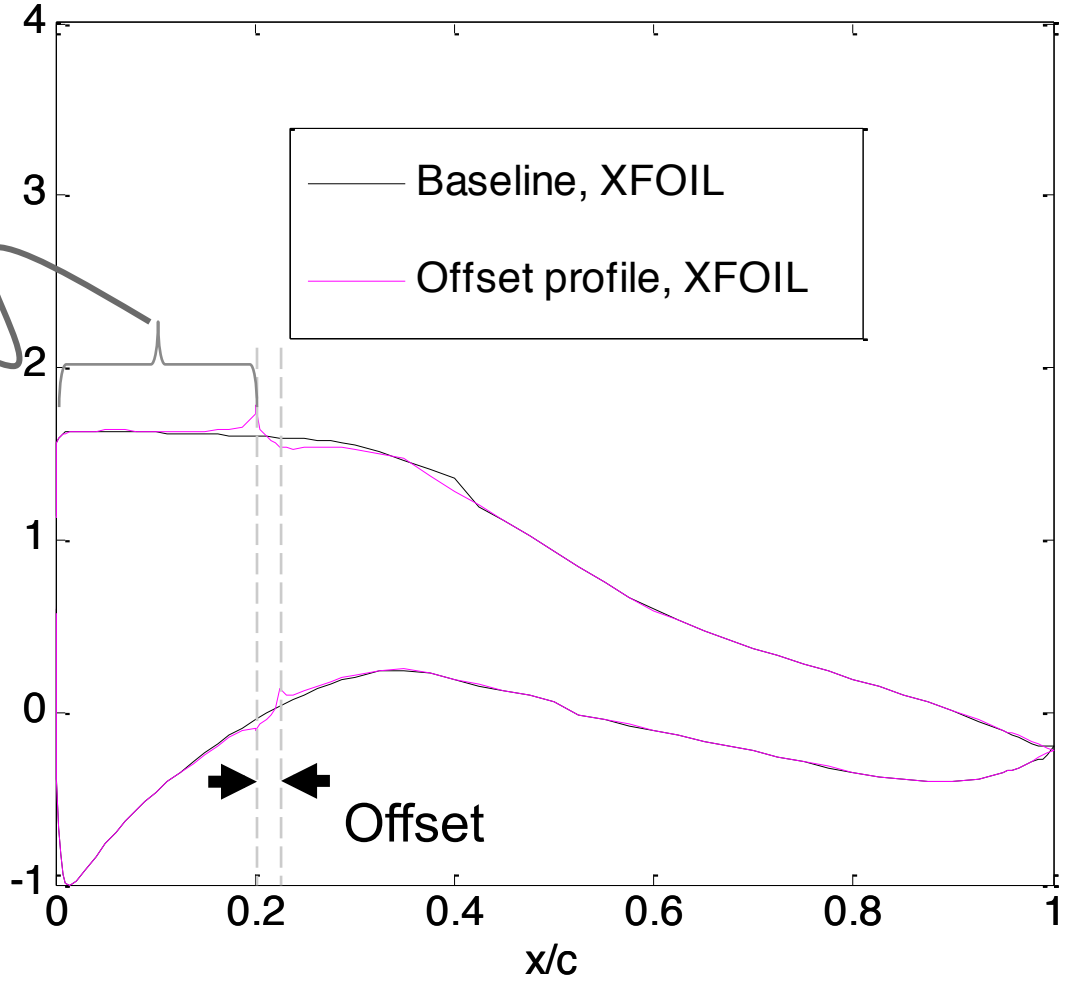

Offset effect predominantly at nose

Misaligned sections: results

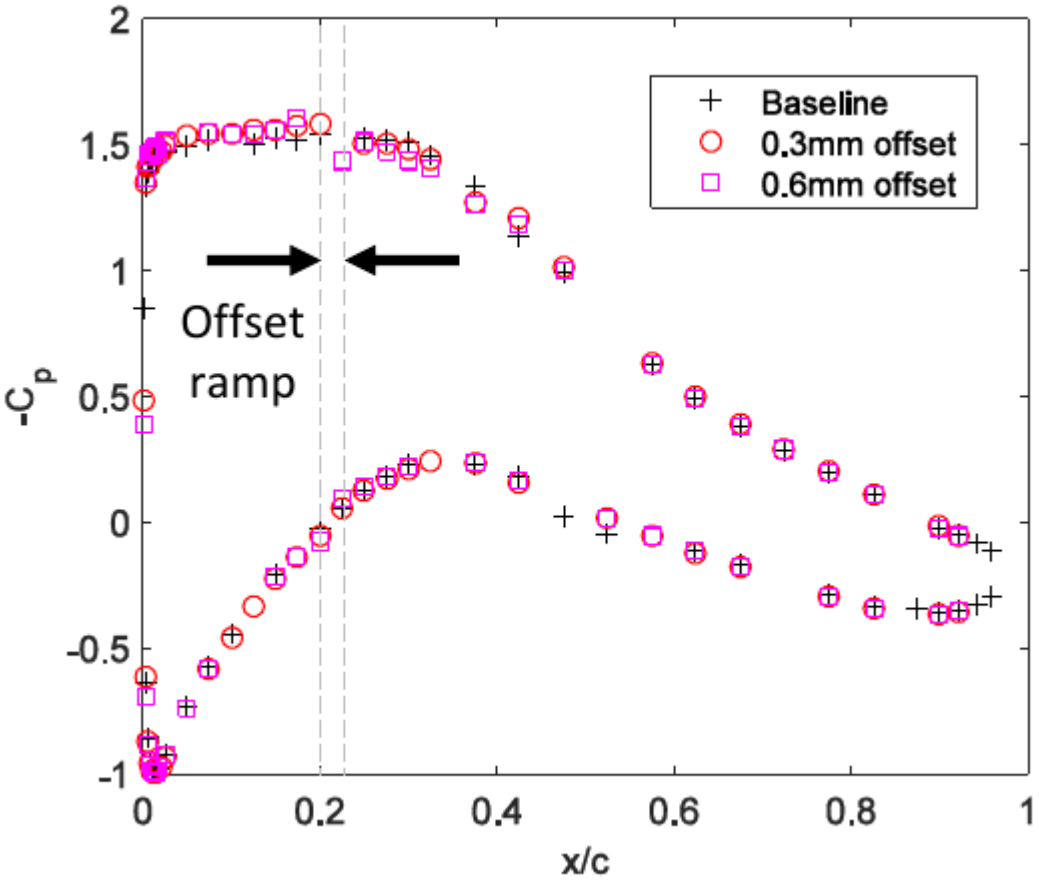

Misaligned sections: results

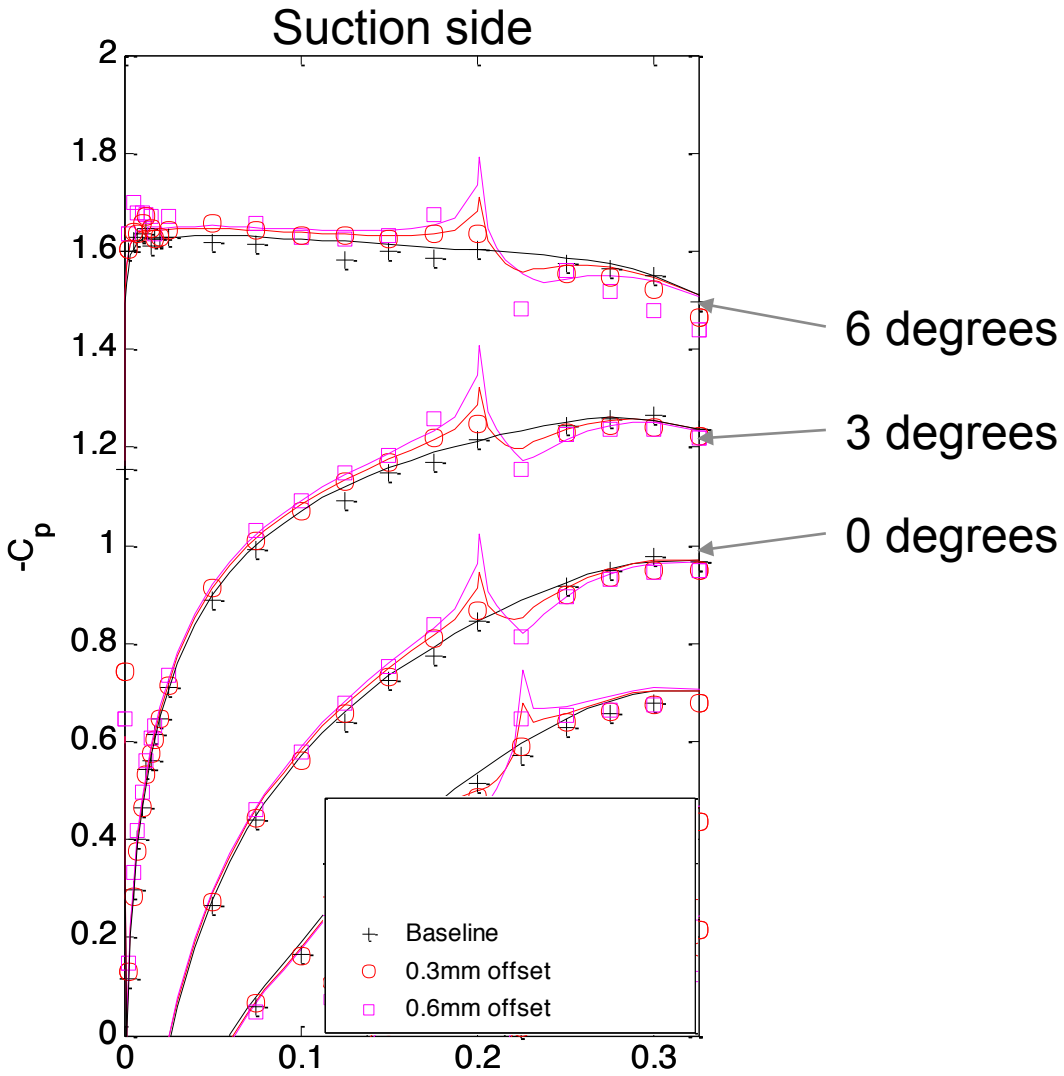

Misaligned sections: results

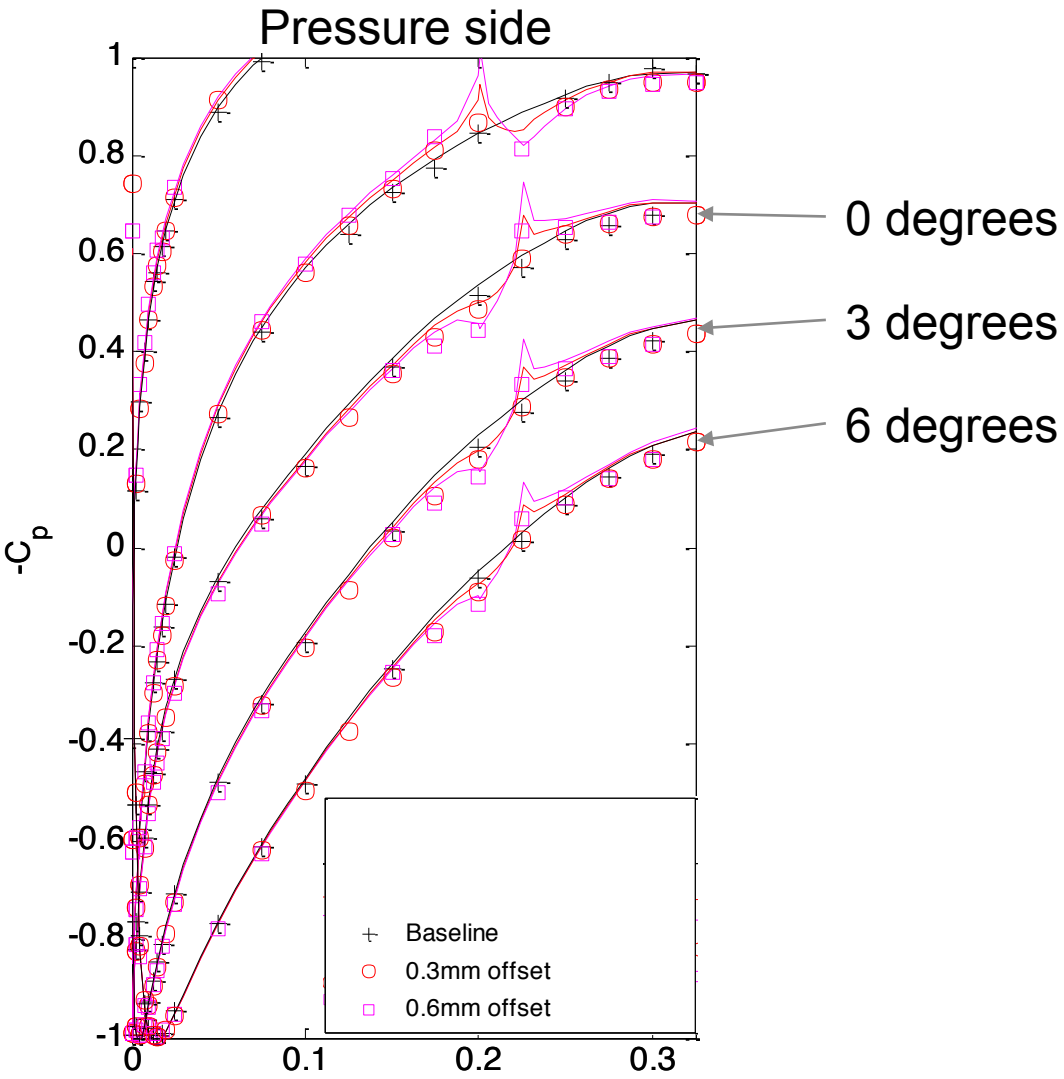

Boundary layer comparison at 6 deg. (from XFOIL)

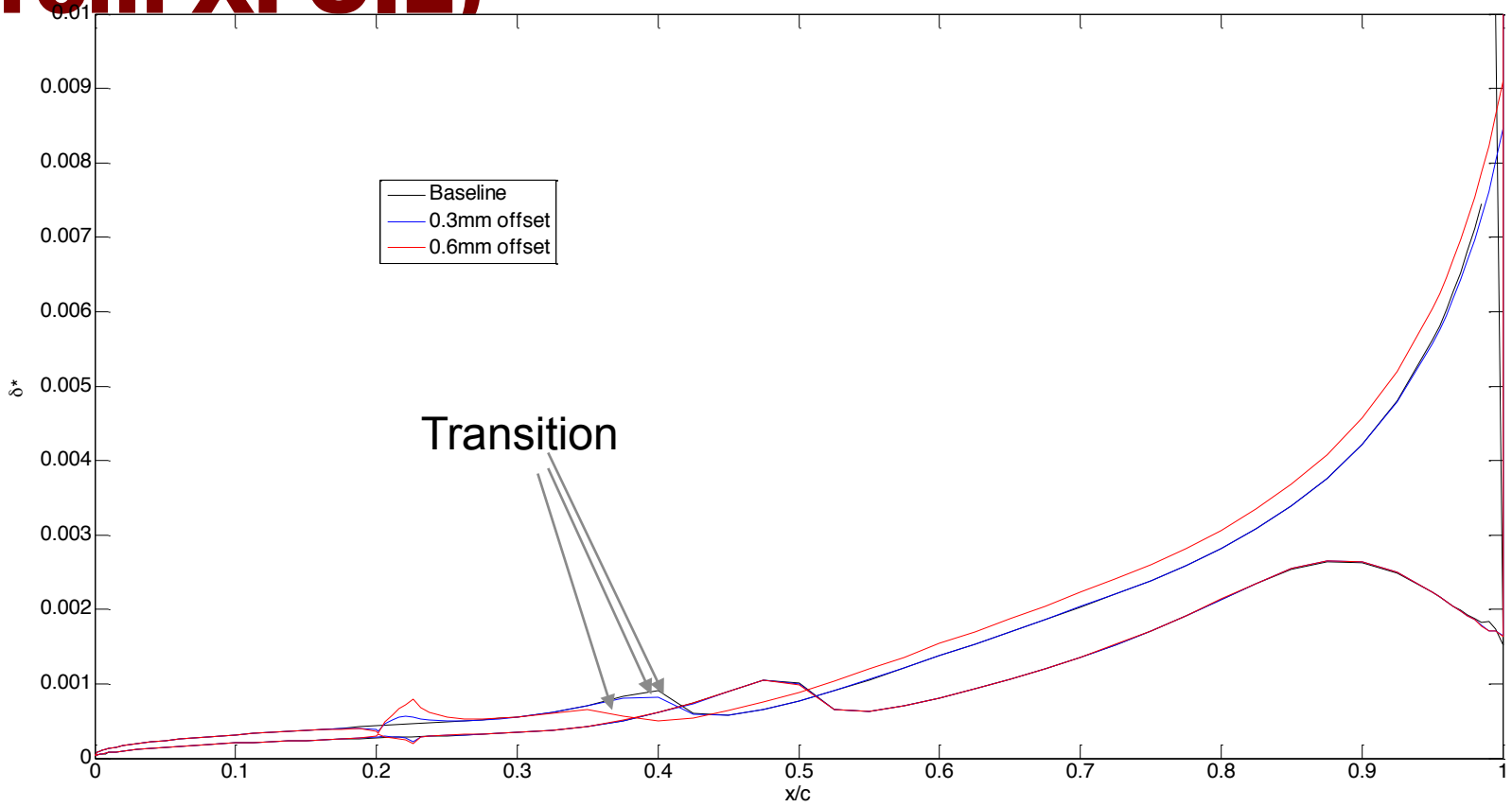

Boundary layer comparison at 7 deg. (from XFOIL)

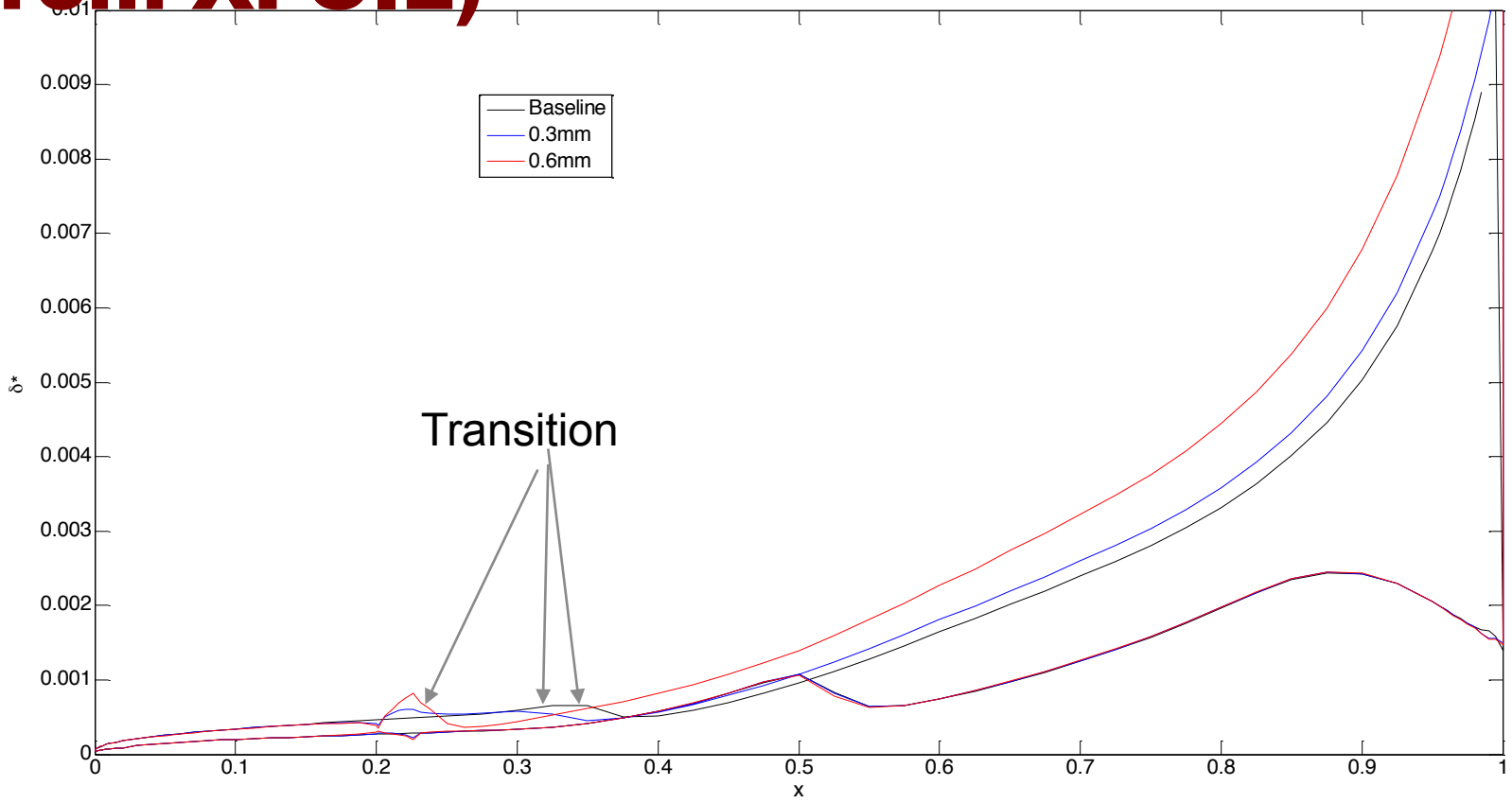

Boundary layer comparison at 8 deg. (from XFOIL)

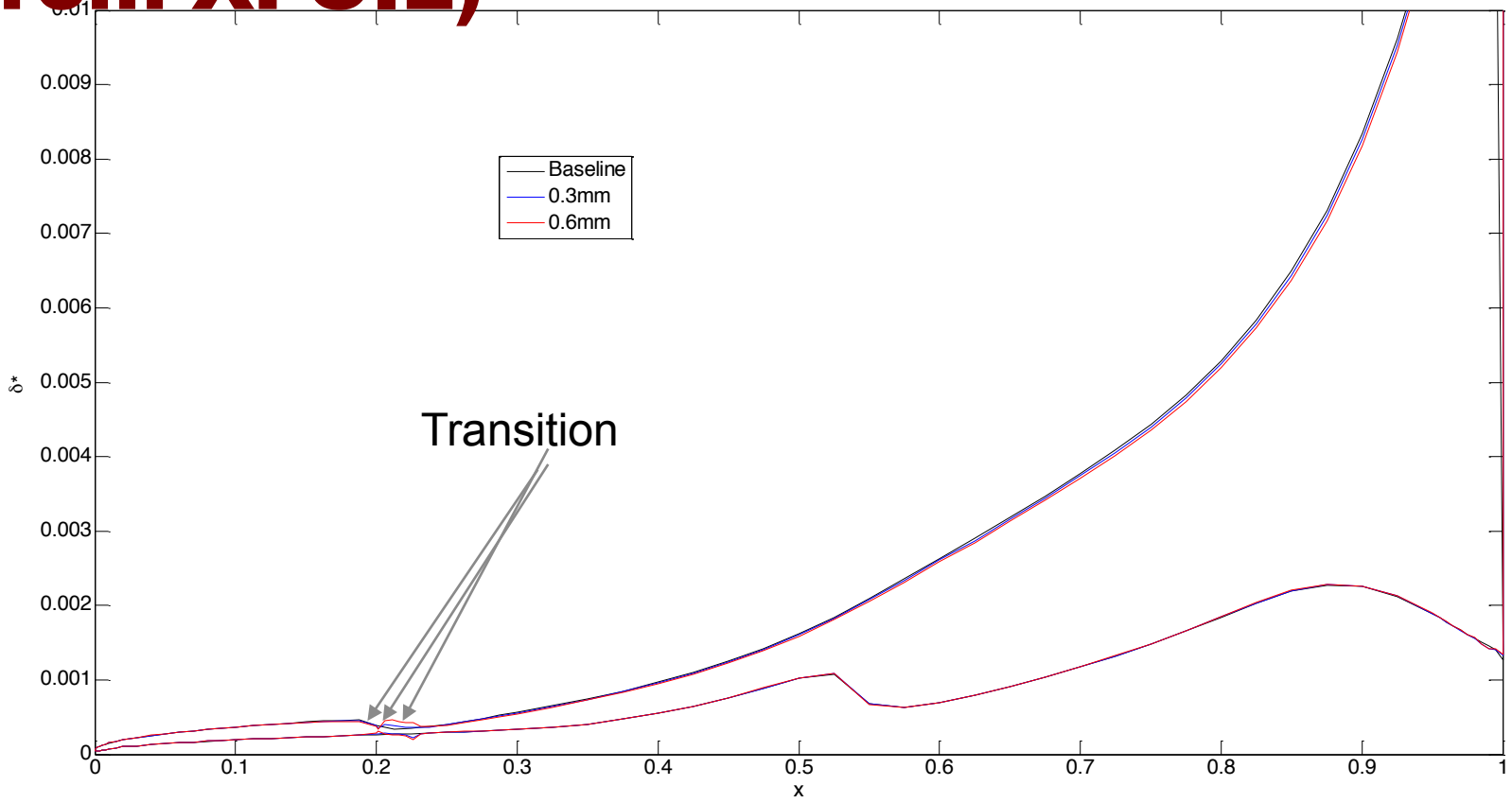

Misaligned sections: results

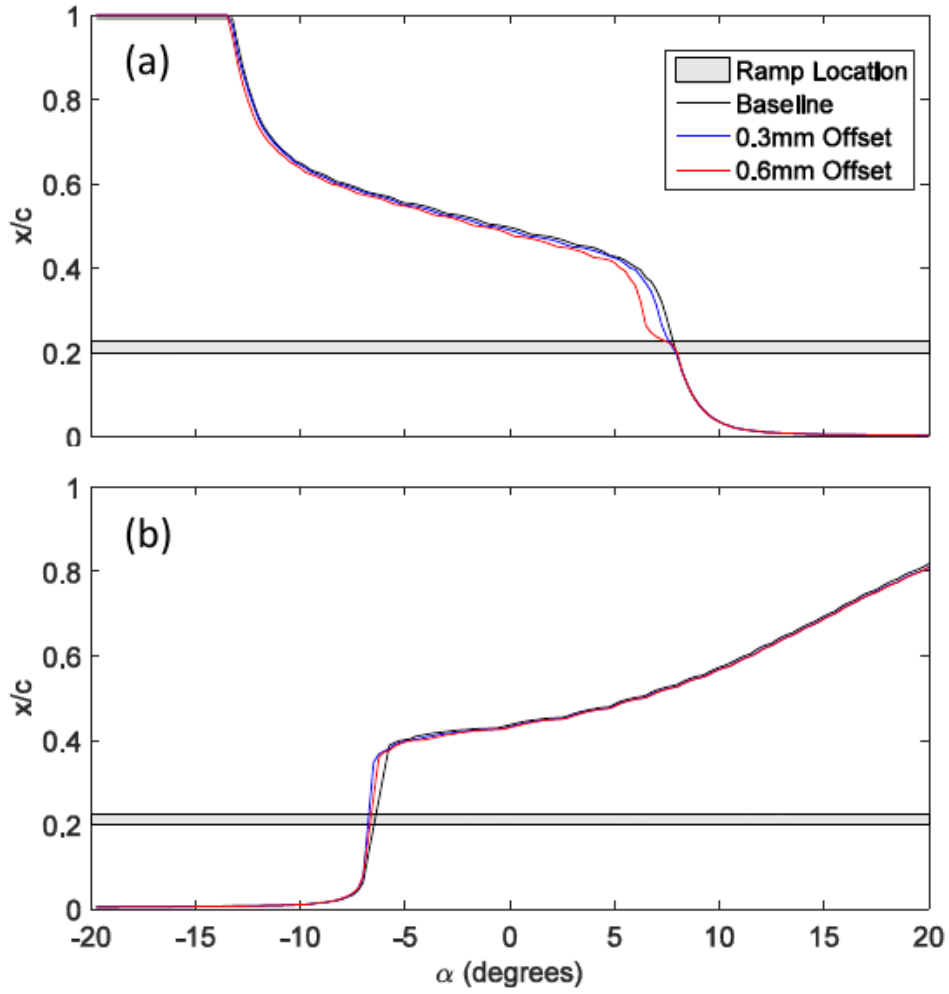

DU91

Fabric sections: literature

Smith and Shyy[18] note that the static aeroelastic problem for a single membrane in two-dimensions can be fully described by five non-dimensional variables: Reynolds number, angle of attack, excess ratio (equal to zero for a taut membrane), non-dimensionalized elastic modulus

$$\Pi_1 = (Eh/q_\infty c)^{1/3} \tag{2}$$

and non-dimensionalized pres-stress

$$\Pi_2 = (Sh/q_\infty c)^{1/3} \tag{3}$$

where E is the elastic modulus of the membrane, S is the pre-stress of the membrane, h is the thickness of the membrane, q_∞ is the dynamic pressure of the freestream flow, and c is the chord of the wing. Depending on whether the membrane tension is dominated by pre-stress or elastic stress, the relative importance of Π_1 versus Π_2 in the out-of-plane equilibrium are interchanged.

Fabric sections: configuration

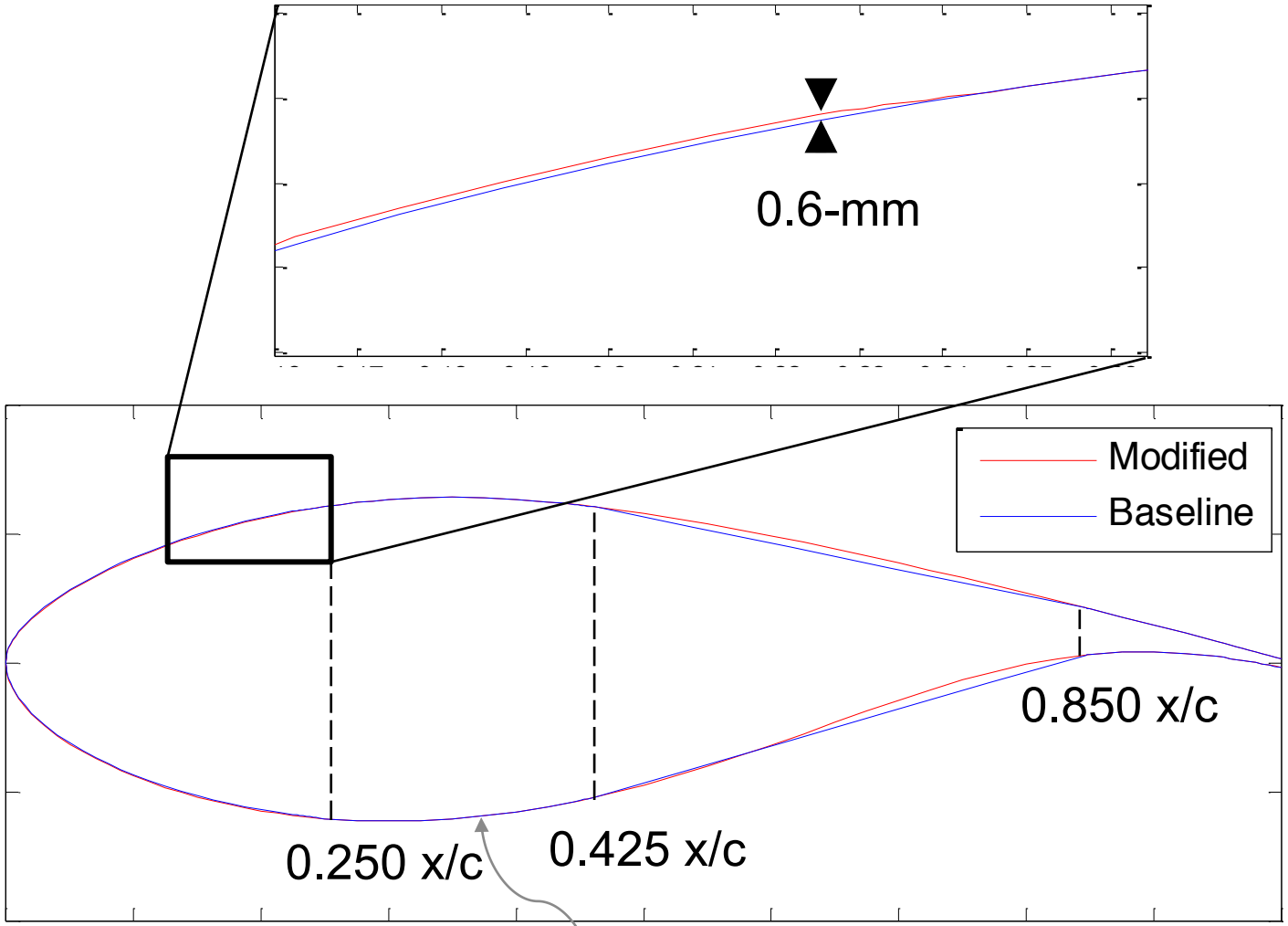

Fabric sections: configuration

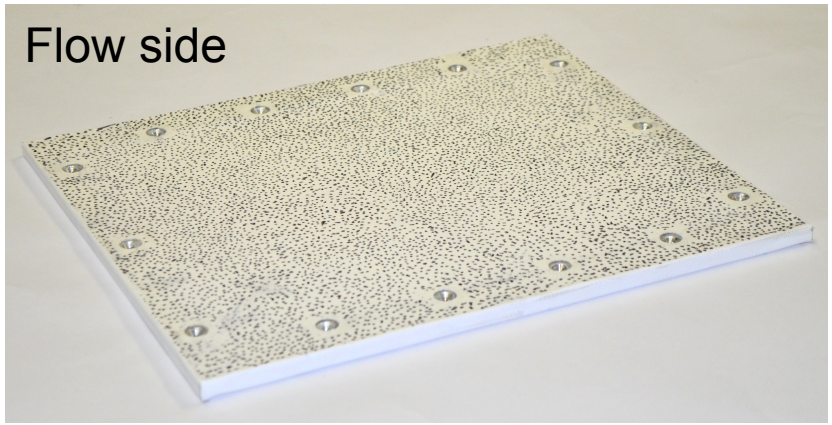

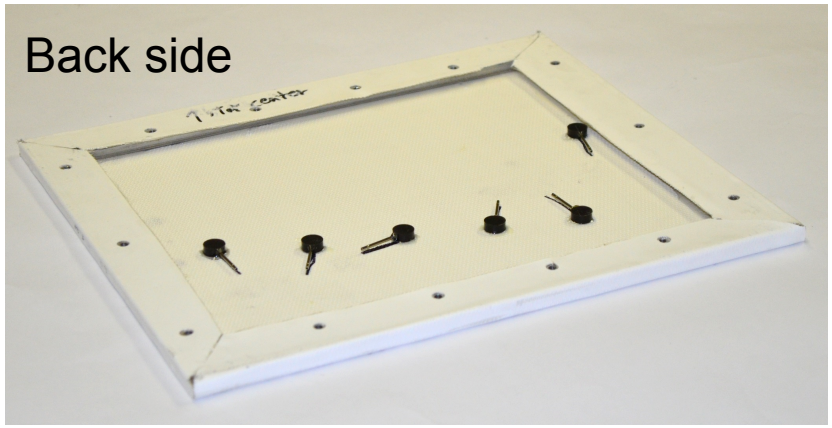

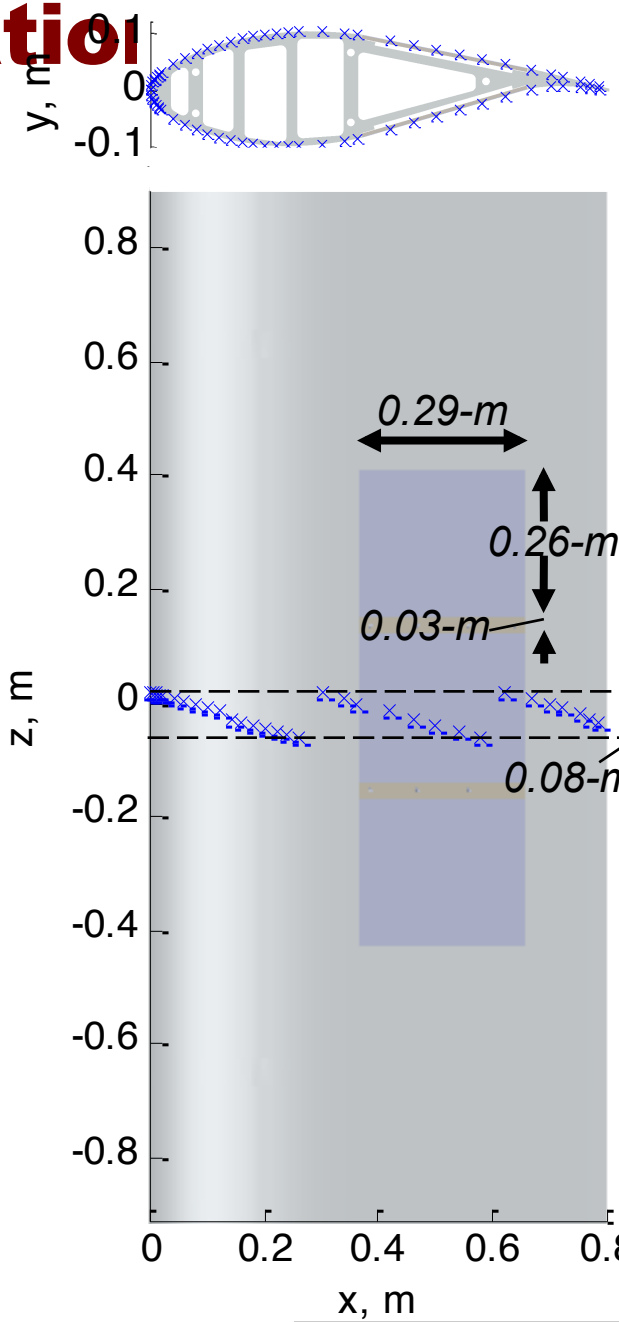

Fabric sections: setup

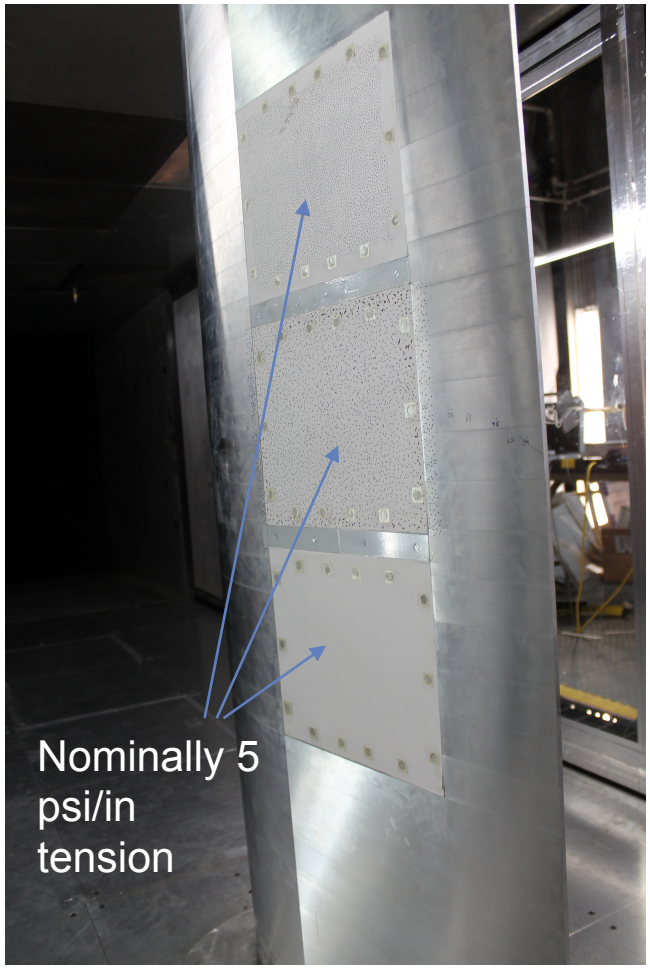

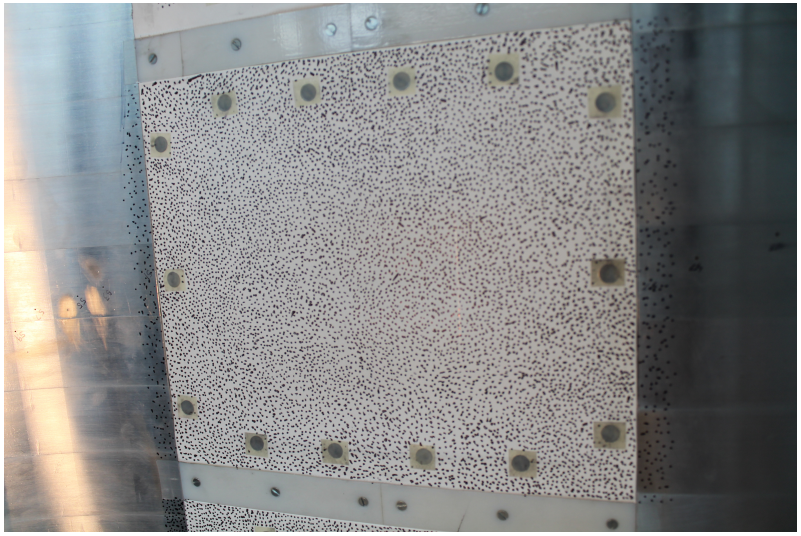

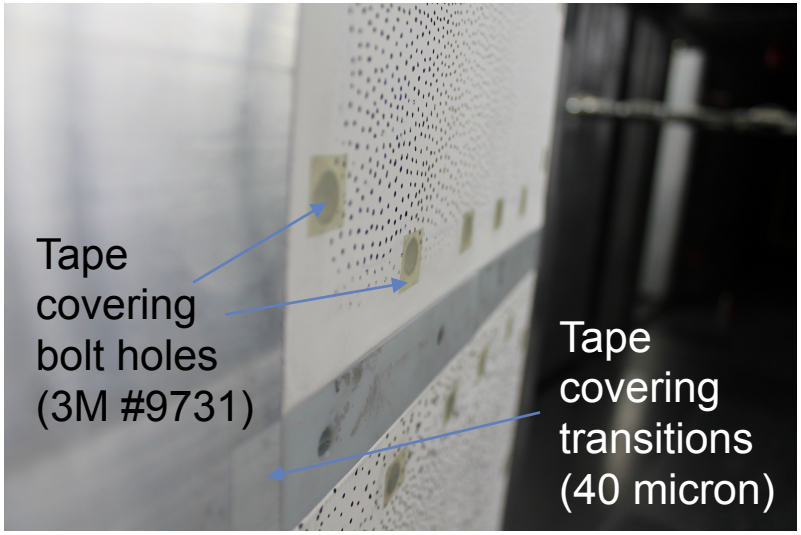

No taping on leading or trailing edges of fabric panels

Fabric sections: setup

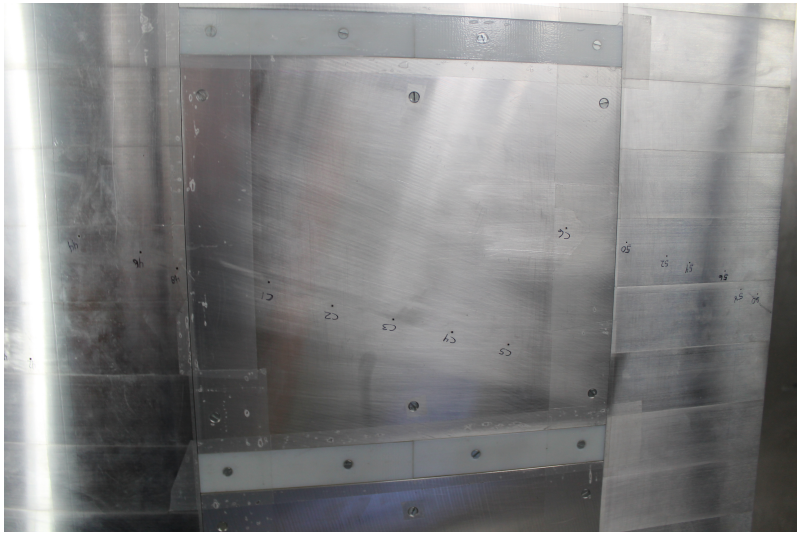

All panel joints covered with 40 micron tape

Fabric sections: setup

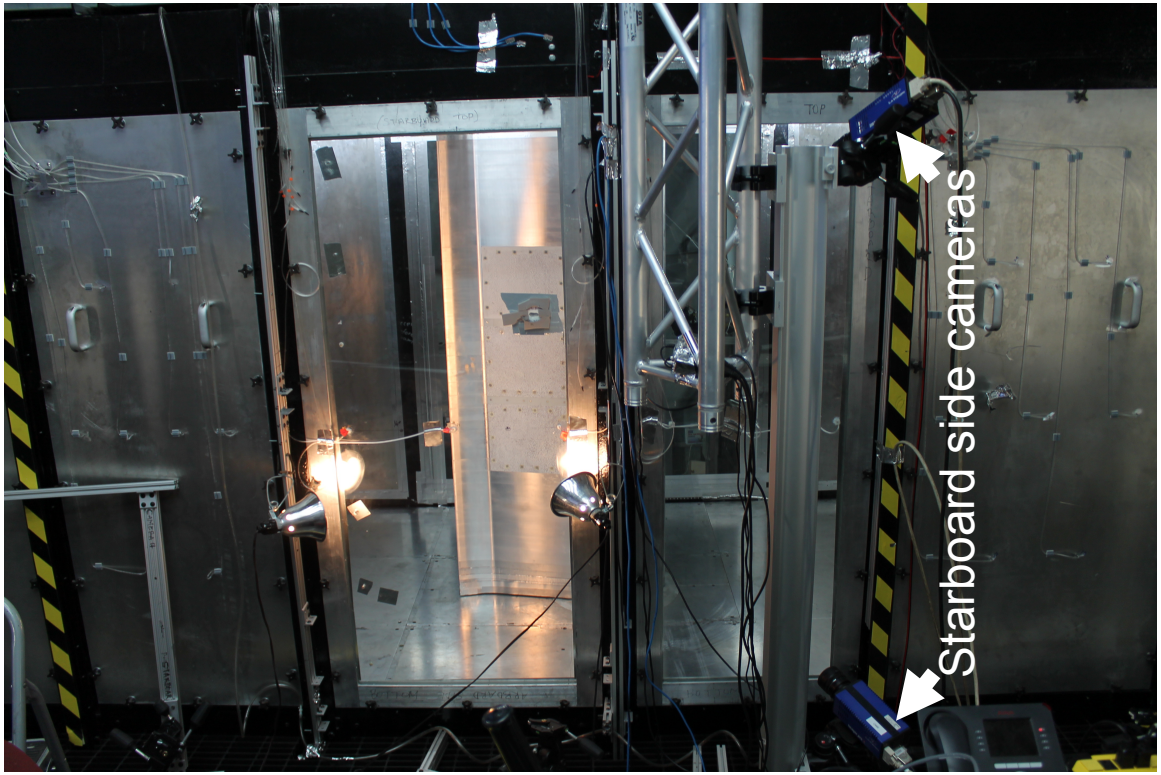

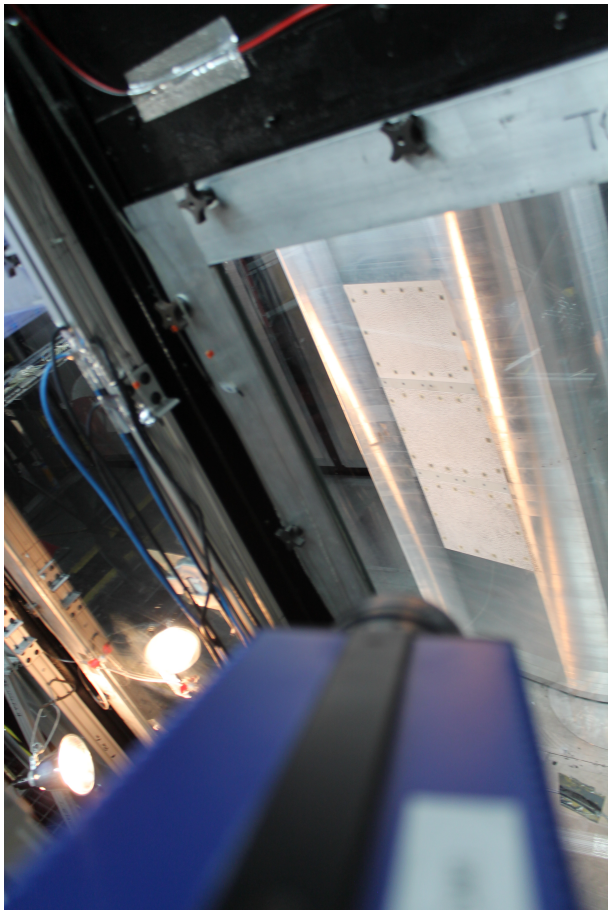

Successful Digital Image Correlation measurements

Design of DIC System

Experimental setup variables:

- b – baseline separation of cameras
- z – depth to measurement space
- f – lens' focal length
- m = magnification
- N – f-stop number ($f/aperture$)
- Δd – physical pixel spacing
- h –number of pixels in 1D
- FOV (field-of-view) –extent of measurement space in 1D
- DOF (depth-of-field) – out-of-plane distance in-focus

Post-processing variables:

- H – circle of confusion diameter

$$\Delta z = z^2(\Delta d)/(bf + z(\Delta d)) \Rightarrow 0.26\ mm$$

$$DOF = -2HN(m+1)/m^2 \Rightarrow 0.42\ m$$

LaVision StrainMaster 2D/3D DIC system:

- 2 Imager Pro X 4M
- 4 MP cameras
- 52-mm lenses
- 2,048-by-2,048 resolution
- 7.4-by-7.4 μm pixel spacing
- 14 Hz sampling
- 14 bit digital output

Starboard-side

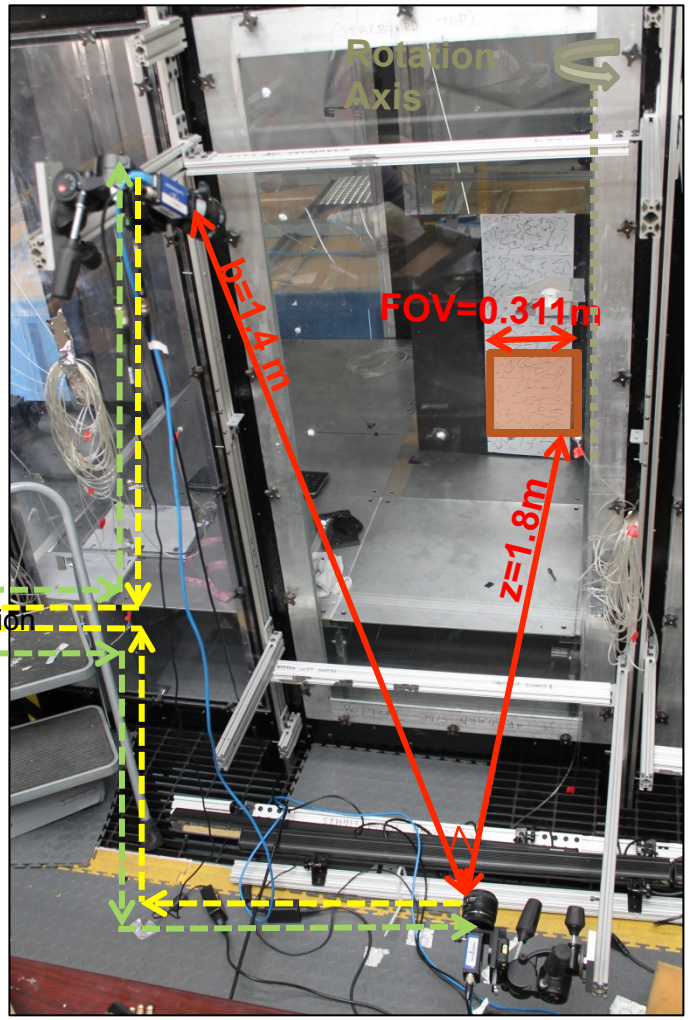

Iteration on Design

for Rotating Truss-Mounted Cameras

$f = hz(\Delta d)/FOV + h(\Delta d) \Rightarrow 24.03\ mm$

$\Delta z = -z^2\ (\Delta d)/(bf + z(\Delta d)) \Rightarrow 0.66\ mm$

$DOF = -2HN(m+1)/m^2 > 10\ cm$ (if aperture < $6mm$)

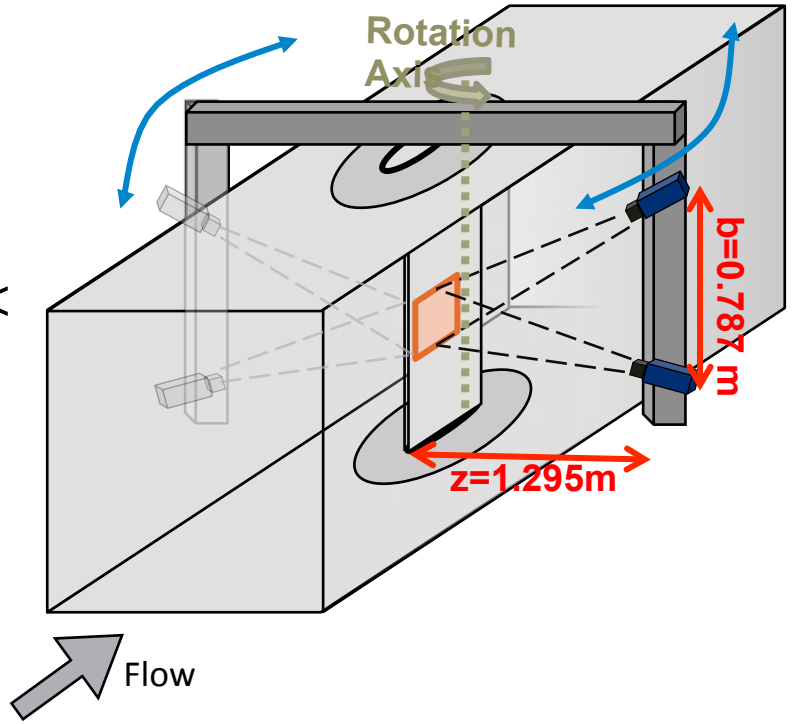

Iteration on Design

for Rotating Truss-Mounted Cameras

$f = hz(\Delta d)/FOV + h(\Delta d) \Rightarrow 24.03\ mm$

$\Delta z = -z^2\ (\Delta d)/(bf + z(\Delta d)) \Rightarrow 0.66\ mm$

$DOF = -2HN(m+1)/m^2\ > 10\ cm$ (if aperture < $6mm$)

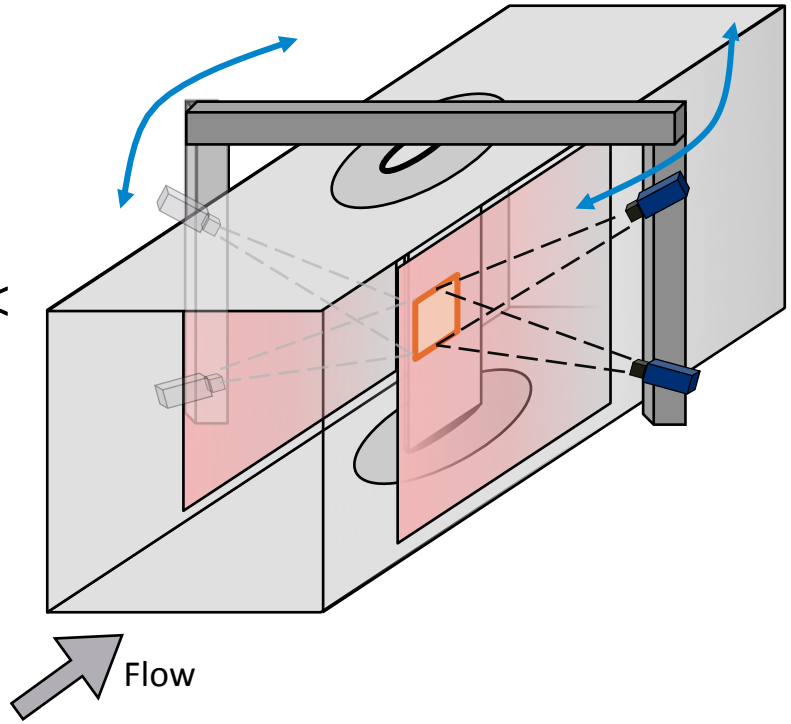

New Side Windows (½" thick laminated glass)

- Uncertainty due to glass refraction:
  Sutton and McFadden (2000): water tunnel experiment, rotation of the cameras of 12 degrees relative to viewing window induced a strain error of 10,000 μstrain or 0.01 m/m
- Structural integrity of glass:
  Viewing angle requirement on dimensions:
  1.42 m streamwise by 1.60 m spanwise (as measured by Tim Meyers)

Fabric sections: results
Re = 3.5M -> 0 (70 m/s ->0)

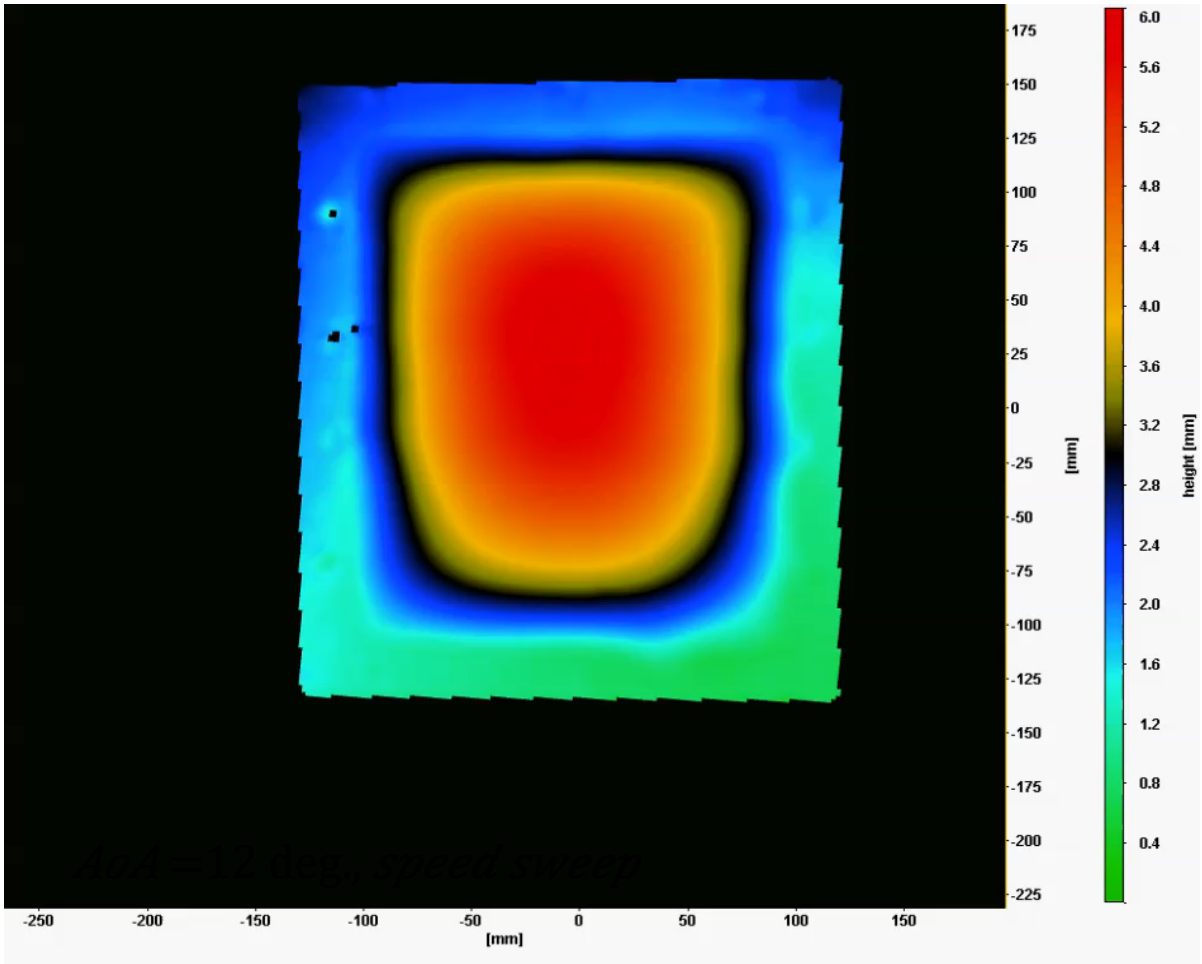

Fabric sections: results

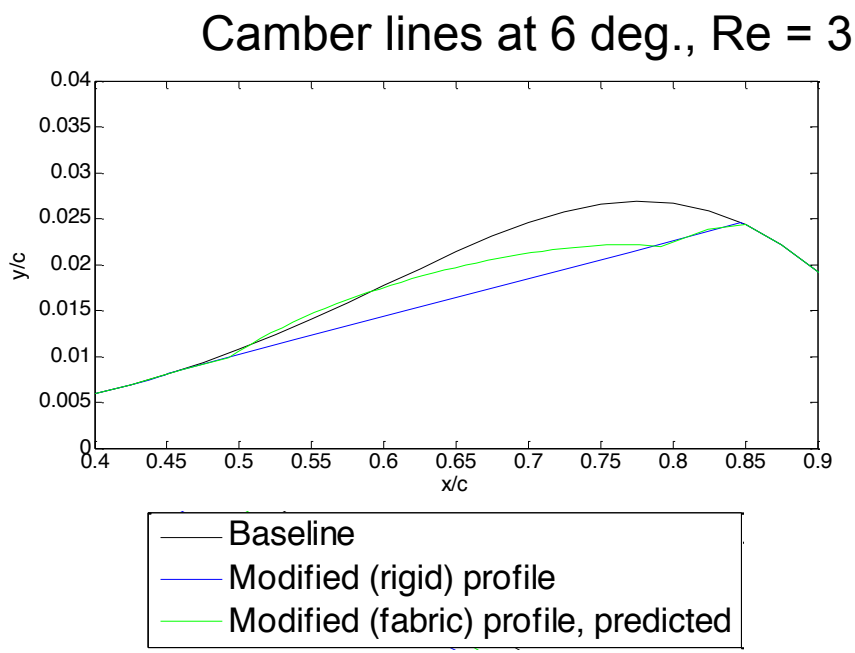

Fabric sections: results

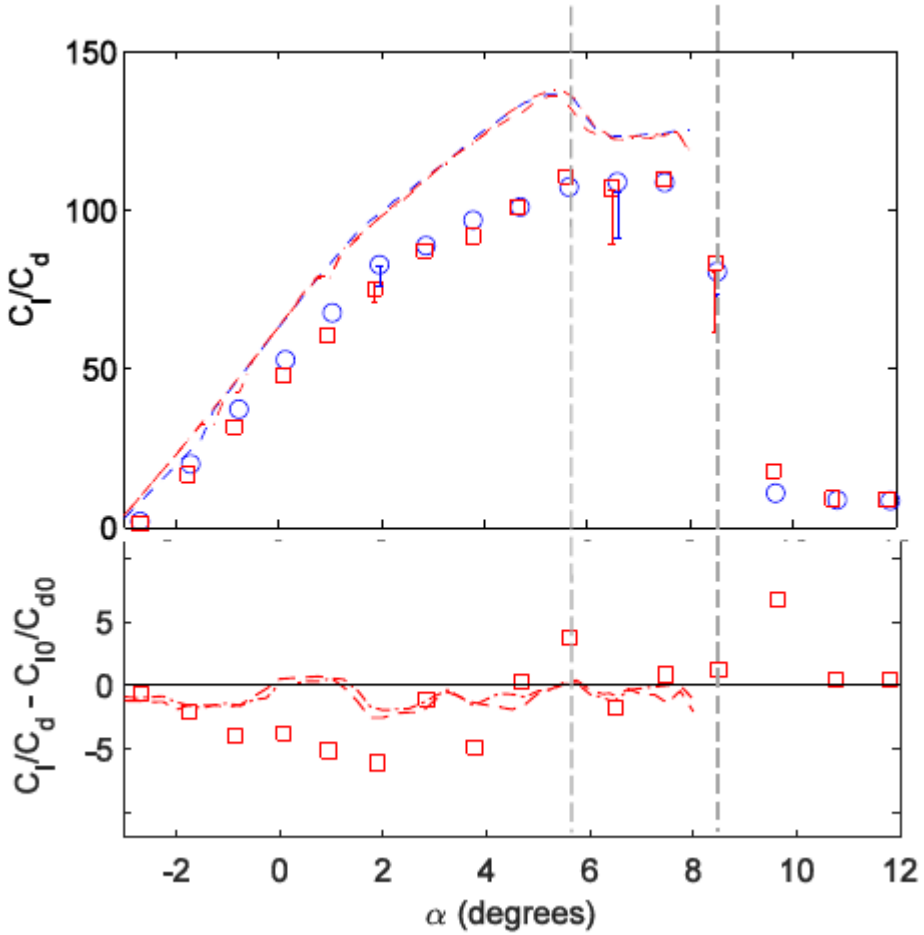

Fabric sections: results

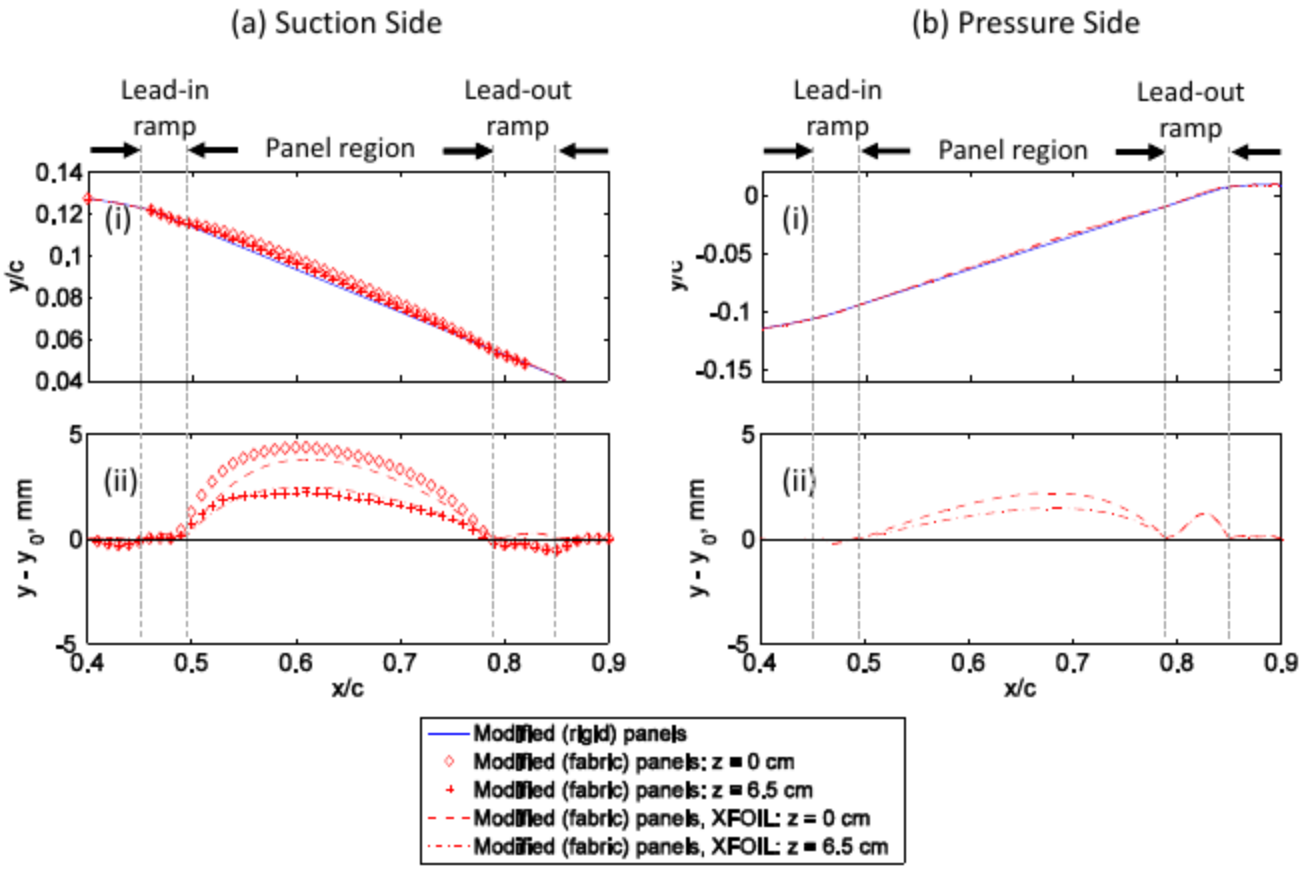

Fabric sections: results

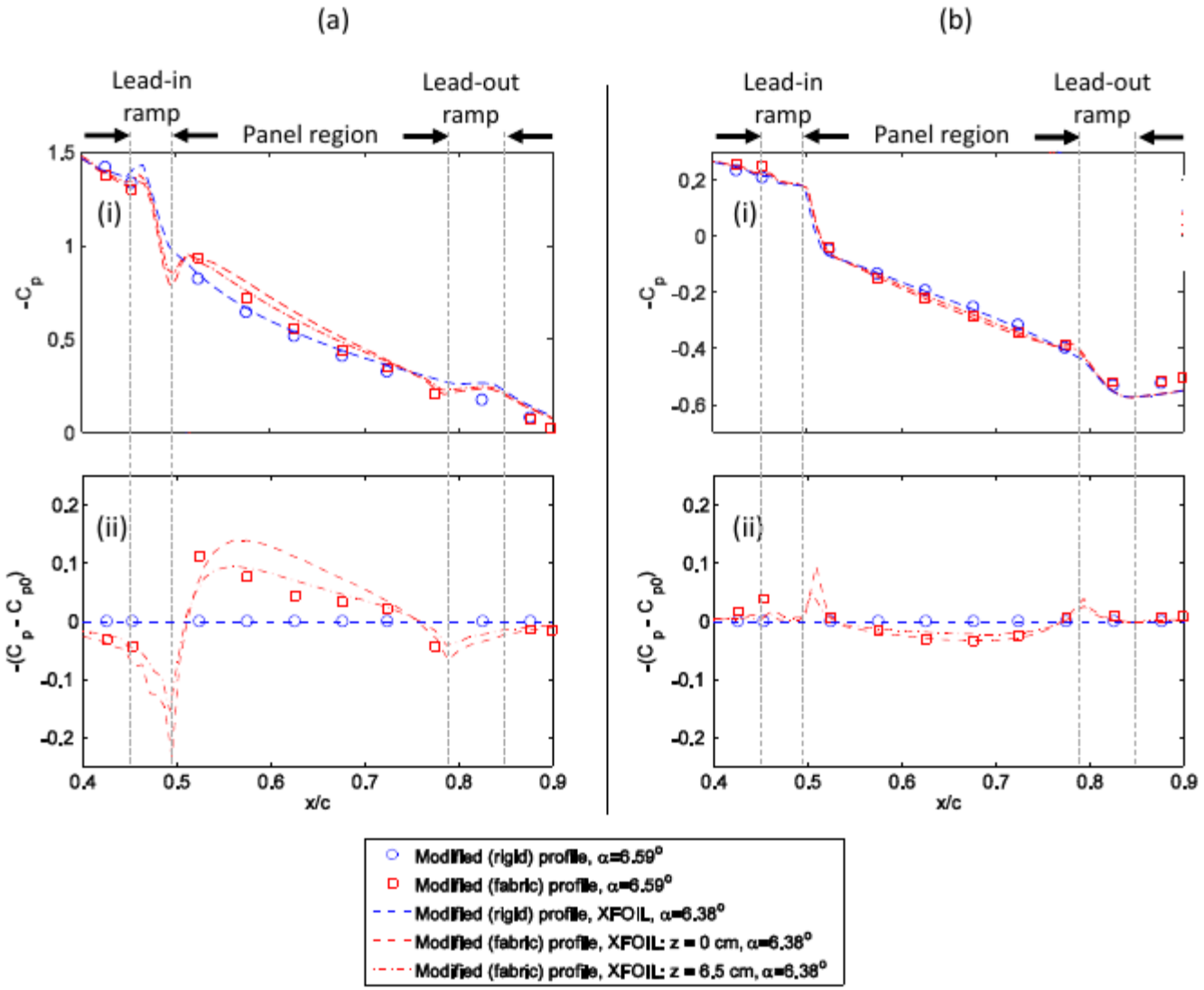

Fabric sections: results

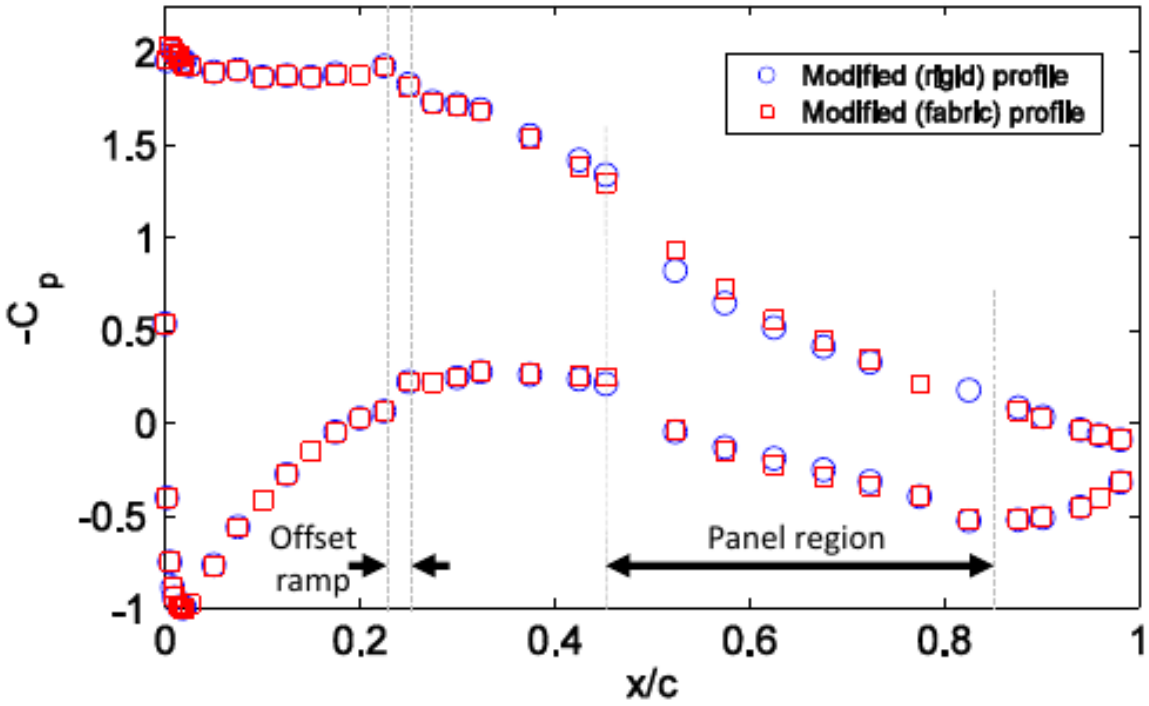

Fabric sections: results

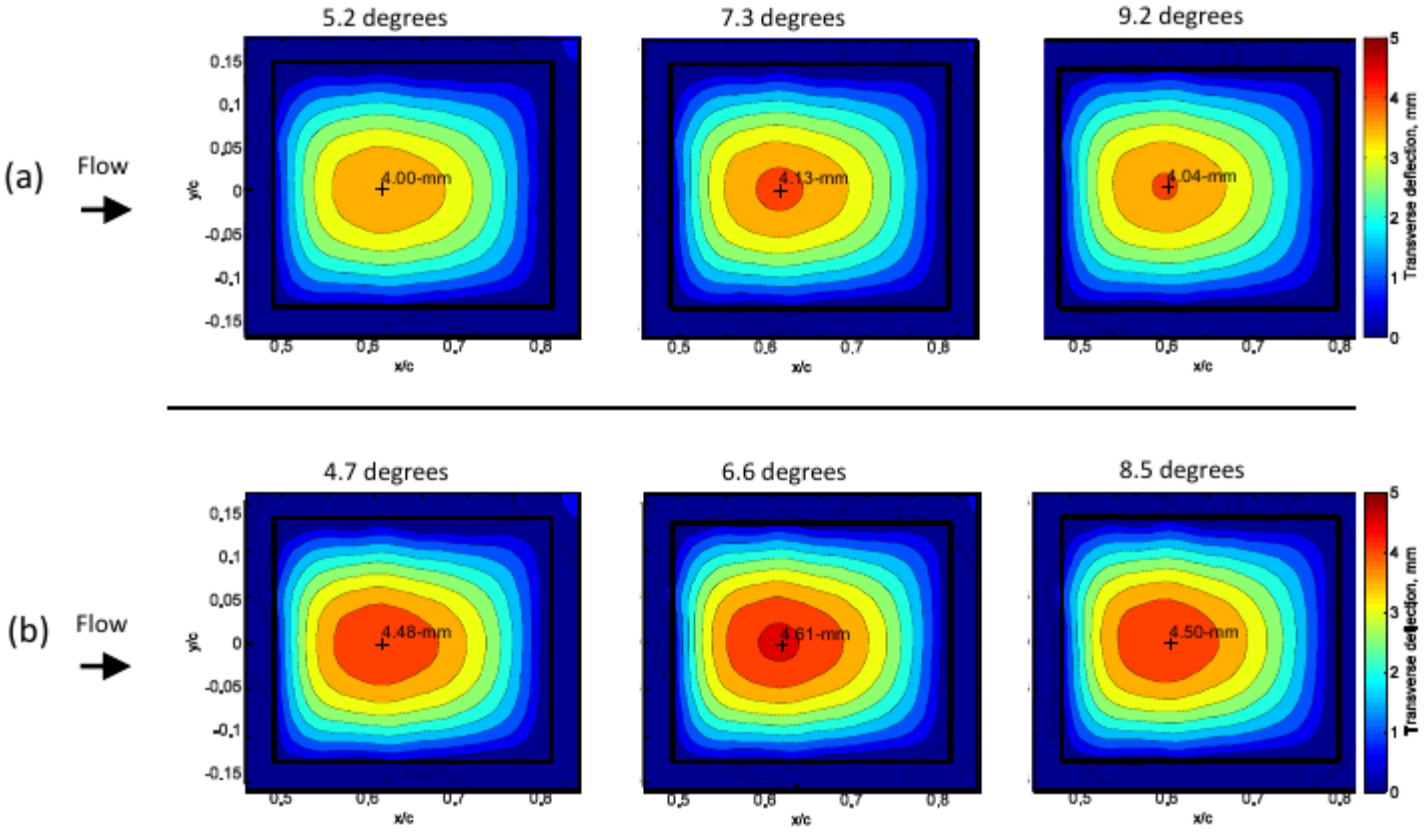

Fabric sections: results

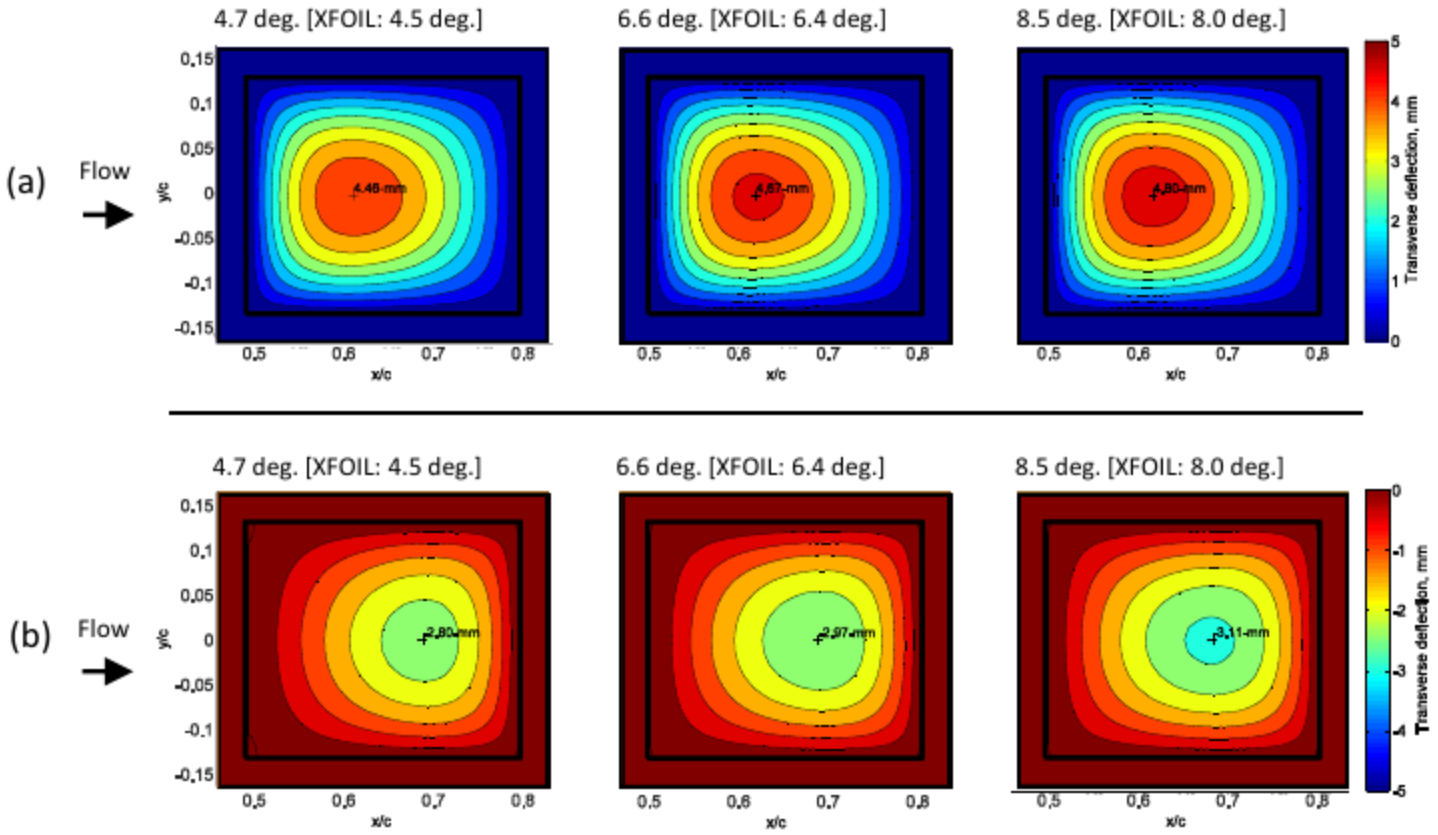

Fabric sections: results

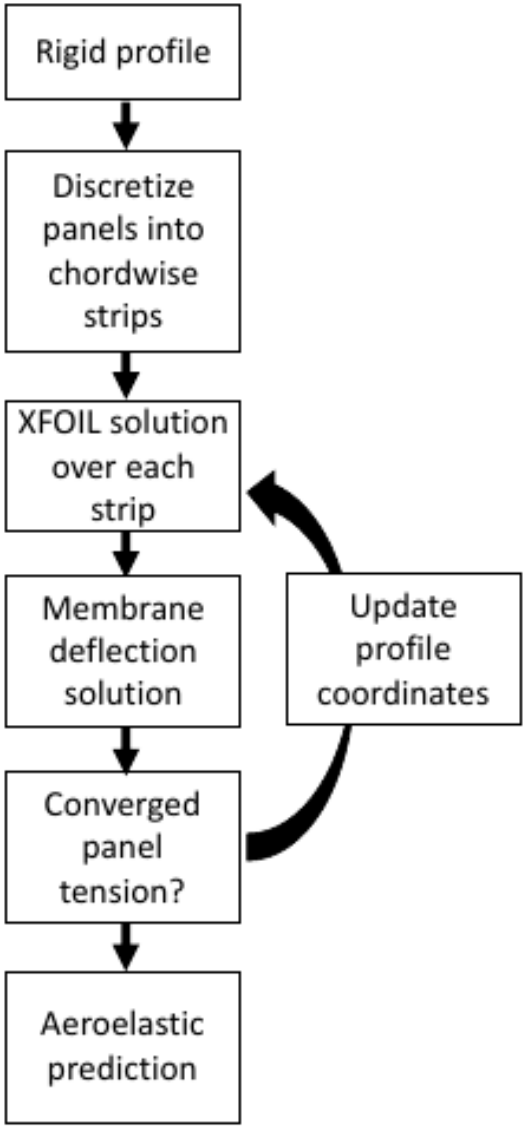

http://www.thonline.com/news/breaking/article_fe7deb6c-c8d5-11e0-9ab6-001a4bcf6878.html